coatings

MDPI

Review

Implantable Thin Film Devices as Brain-Computer Interfaces: Recent Advances in Design and Fabrication Approaches

Yuhao Zhou [1], Bowen Ji [1,2,*], Minghao Wang [3], Kai Zhang [2], Shuaiqi Huangfu [1], Huicheng Feng [1,2], Honglong Chang [1,2] and Xichen Yuan [2,*]

[1] Unmanned System Research Institute, Northwestern Polytechnical University, Xi'an 710072, China; zyh160@mail.nwpu.edu.cn (Y.Z.); hfsq@mail.nwpu.edu.cn (S.H.); hfeng@nwpu.edu.cn (H.F.); changhl@nwpu.edu.cn (H.C.)
[2] Ministry of Education Key Laboratory of Micro and Nano Systems for Aerospace, School of Mechanical Engineering, Northwestern Polytechnical University, Xi'an 710072, China; zhangkai0302@mail.nwpu.edu.cn
[3] College of Electronics and Information, Hangzhou Dianzi University, Hangzhou 310018, China; mhwang@hdu.edu.cn
* Correspondence: bwji@nwpu.edu.cn (B.J); xichen.yuan@nwpu.edu.cn (X.Y.)

Abstract: Remarkable progress has been made in the high resolution, biocompatibility, durability and stretchability for the implantable brain-computer interface (BCI) in the last decades. Due to the inevitable damage of brain tissue caused by traditional rigid devices, the thin film devices are developing rapidly and attracting considerable attention, with continuous progress in flexible materials and non-silicon micro/nano fabrication methods. Therefore, it is necessary to systematically summarize the recent development of implantable thin film devices for acquiring brain information. This brief review subdivides the flexible thin film devices into the following four categories: planar, open-mesh, probe, and micro-wire layouts. In addition, an overview of the fabrication approaches is also presented. Traditional lithography and state-of-the-art processing methods are discussed for the key issue of high-resolution. Special substrates and interconnects are also highlighted with varied materials and fabrication routines. In conclusion, a discussion of the remaining obstacles and directions for future research is provided.

Keywords: implantable thin film devices; brain-computer interfaces; structure design; fabrication approaches

check for updates

Citation: Zhou, Y.; Ji, B.; Wang, M.; Zhang, K.; Huangfu, S.; Feng, H.; Chang, H.; Yuan, X. Implantable Thin Film Devices as Brain-Computer Interfaces: Recent Advances in Design and Fabrication Approaches. *Coatings* **2021**, *11*, 204. https://doi.org/10.3390/coatings11020204

Academic Editor: Je Moon Yun

Received: 19 December 2020
Accepted: 7 February 2021
Published: 10 February 2021

Publisher's Note: MDPI stays neutral with regard to jurisdictional claims in published maps and institutional affiliations.

Copyright: © 2021 by the authors. Licensee MDPI, Basel, Switzerland. This article is an open access article distributed under the terms and conditions of the Creative Commons Attribution (CC BY) license (https://creativecommons.org/licenses/by/4.0/).

1. Introduction

Brain-computer interface (BCI) technology shows great value in the clinical treatment of brain diseases—including stroke and epilepsy—and plays a vital role in frontier scientific fields such as brain research, bioelectronics, and nerve prosthetics [1–6]. Implantable BCI, as a common tool to record neural signals in biomedical research, can be divided into cortical electrodes and intracranial penetrating electrodes, according to the different implantation sites [7–16]. Meanwhile, the implantable BCI has expanded many functional features, including the modulation of neural activities by light, electrical and magnetic stimulation, and drug delivery via microfluidics to achieve local control or treatment [17–31]. Most of the existing BCI devices are rigid, such as the Utah electrode arrays, Michigan probes and Pt-Ir microwire electrodes [17,32–41]. The Utah electrode array shows the characteristics of high density, compact layout and reliability, which can collect hundreds of neural signals synchronously. The Michigan electrode is also a needle-type rigid probe, which can support a linear array of recording sites on the shank, whereas the Utah electrode array can each support only one recording site at the tip of each electrode. These rigid invasive electrodes are hardly compatible with the soft brain [42,43], which even may cause severe damage to the brain tissue [44–46]. For the chronic implantation, glial scars are easy to cover the surface of electrode sites, which is one of the reasons that affects the electrophysiological quality of neural signals [47,48]. Traditional silicon and metal materials cannot match well

with the brain tissue due to the stiffness problems. Therefore, it is urgent to develop new BCI devices based on flexible or soft materials with satisfactory mechanical performance, to effectively comply with soft tissue, reduce tissue damage during insertion, and extend the implantation lifetime. In recent years, many cutting-edge research has reported the development of neural interfaces based on the polymer materials, including the polyimide threads as flexible neural probes as proposed by Elon Musk in 2019 [49].

Biocompatibility is an important factor in evaluating a polymer device. A BCI device with good biocompatibility should be soft, nontoxic, and harmless to human body. It is difficult to match the Young's modulus between the traditional rigid materials and soft brain tissues (E = 0.4–15 kPa) [50]. However, flexible polymer devices have unique advantages in mechanical compatibility with soft brain tissue. The Young's modulus of biocompatible polymers such as polyimide (PI) [51,52], Parylene [53,54], SU-8 [55,56], and polyethylene terephthalate (PET) [18,56] is from 2 to 5 GPa for certain types, which is much lower compared to rigid electrodes. Some polymers such as Parylene-C and PDMS are usually used as barrier films to protect the electrodes from moisture penetration, although they are not the ideal encapsulation materials which require long and accelerated tests against body fluid. Meanwhile, flexible thin film devices can be combined with optical stimulation modules based on optogenetics, which combines genetic engineering with light to manipulate the activity of individual nerve cells, including optical fibers [57–59], optical waveguides [60,61] and micro-LEDs [62,63]. In addition, compared with the rigid devices, flexible thin film devices have the following distinct advantages: (1) the structure layout is multiple and variable [64–67]; (2) the polymer films are compatible with micro/nano fabrication processes to realize miniaturization with fine high resolution [68,69]; and (3) the biocompatibility of polymer electrodes ensures the stable chronic in-vivo recording and reduces tissue inflammation [70,71].

In this work, implantable thin film devices with micron-scale size and good flexibility were classified according to the structures and fabrications as illustrated in Figure 1. According to the structure design, flexible neural electrodes can be divided into four categories: planar [69,72], mesh [73,74], probe [49,75], and micro-wire [64,76] layouts. Different structures can be applied to the specific implantation locations, which will affect the tensile property, spatial resolution, and integration. The development of various structures is beneficial for the detection of neural signals at different depths, the enrichment of electrode types, and multifunctional integration. The fabrication processes of flexible thin film devices mainly focuses on the following three aspects: high resolution [68,77], special substrates [78,79], and special interconnects [80,81]. Traditional lithography process and other new approaches were summarized to realize high-resolution aspects. Compared with widely used materials such as PI, Parylene, Polydimethylsiloxane (PDMS), etc., new materials—such as biodegradable materials, shape memory polymers, bacterial cellulose, etc.—can also be applied as substrates with unique characteristics. In addition to traditional conductive metals such as gold and platinum, new conductive materials can provide special properties such as high transparency and high stretchability. Finally, challenges and future developments will be discussed based on recent advances in design and fabrication approaches of the implantable thin film BCI devices.

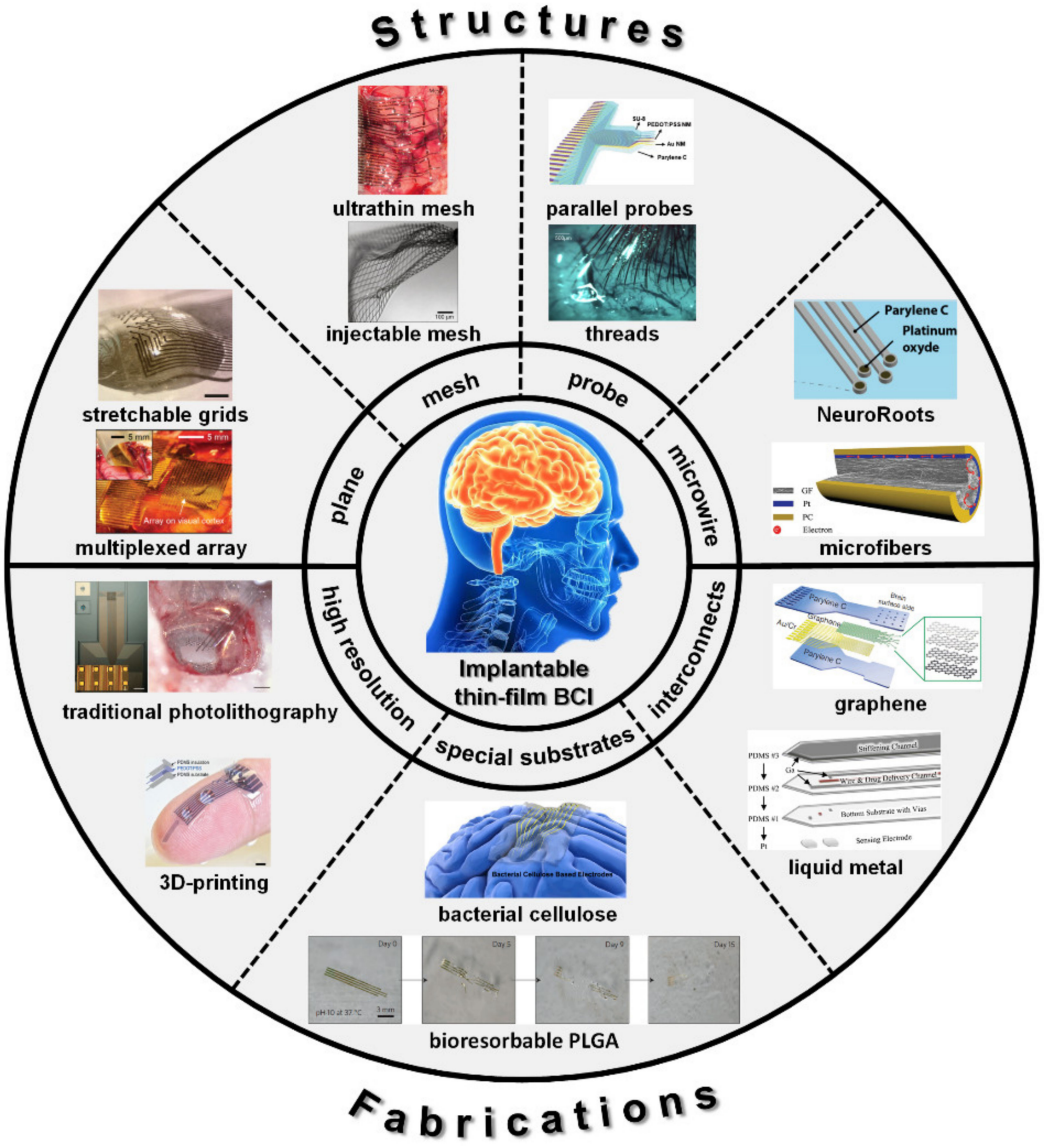

Figure 1. Classification of implantable thin film devices as Brain-computer interface (BCI) according to the four structure layouts and three fabrication approaches (reprinted with permissions from [49,68,69,72–74,76–83]).

2. Design

2.1. Planar Layout

Thin film devices with planar layout can record neural signals from the surface of the cerebral cortex. Owing to the entire planar substrate, high-density electrode sites can be distributed throughout the region with enough space for interconnects. The main efforts are focused on the ultra-thin flexible materials for conformal attachment and soft materials with stretchability to achieve more compliant results with soft tissue. Figure 2 shows some recent works of planar layout, which can be divided into flexible and soft structures according to the different substrate materials.

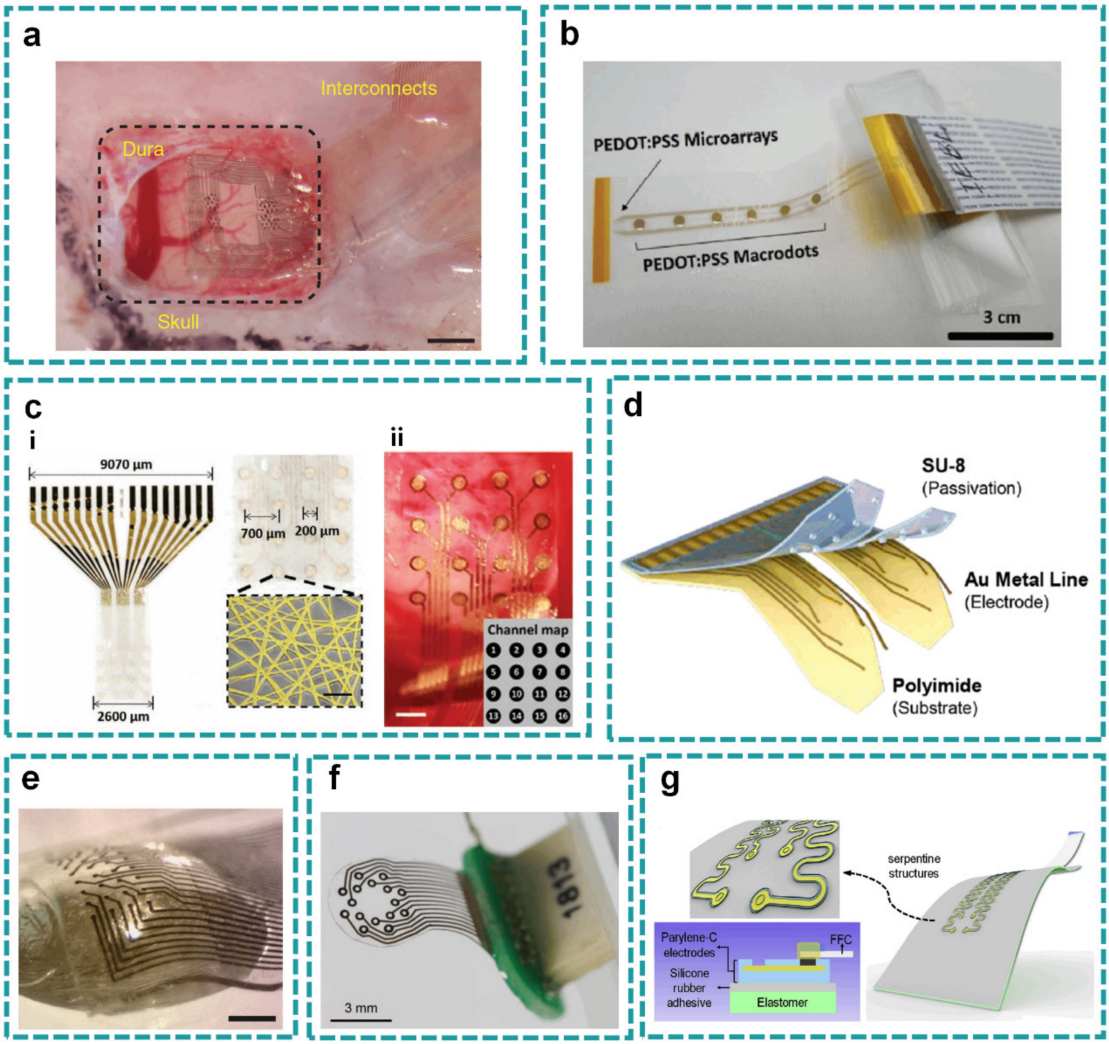

Figure 2. Planar layout. (**a**) a representative flat ultrathin electrode array with good biocompatibility, high density and ultra-thin thickness; scale bar, 1mm (reprinted with permission from [68]); (**b**) a parylene-based planar array with 56 microelectrodes and 6 macrodots (reprinted with permission from [84]); (**c**) an Au NN-based transparent ECoG monitoring system proposed as implantable planar neural electrodes; i: scale bar, 5 μm; ii: scale bar, 500 μm (reprinted with permission from [85]); (**d**) a flexible planar microelectrode device which could be inserted through a small cranial suture (reprinted with permission from [56]); (**e**) a soft, high-density and stretchable electrode grid (SEG) based on an inert, high-performance composite material; scale bar, 500 μm (reprinted with permission from [72]); (**f**) a PDMS-based soft, stretchable, 16-channel planar ECoG array (reprinted with permission from [86]); (**g**) the serpentine conductive leads embedded in polymer films attached on any soft planar substrate as the stretchable planar ECoG electrodes (reprinted with permission from [87]).

2.1.1. Flexible Planar Structure

Polymers are most widely used as the flexible substrates with planar layout, which have good mechanical fatigue resistance for chronic implantation on the cortical surface. A representative flat ultrathin electrode array called NeuroGrid was designed with the general characteristics of flexible thin film devices: good biocompatibility, high density, and ultra-thin thickness of 4 μm (Figure 2a) [68]. The NeuroGrid was designed with ultra-small electrode sites, which could successfully record stable local field potential and action potential from the surface cortical neurons without penetrating into the brain for more than one week. In another work, high-density Neural Matrix electrodes were designed for a long service life of 60 years [88]. Meanwhile, it is also worth mentioning that researchers used thermally grown silicon dioxide (t-SiO_2) as a barrier on both sides with moisture-proof effect.

The impedance will increase as the electrode site downscales to improve spatial specificity, thus modification is necessary to increase the SNR (signal-to-noise ratio). Mehran et al. compared the performance of poly(3,4-ethylenedioxythiophene) poly(styrenesulfonate) (PEDOT:PSS) electrodes and traditional platinum electrodes (Figure 2b) [84]. They made a microelectrode array with 56 microelectrodes and 6 microdots modified by PEDOT:PSS on the thin planar substrate of Parylene-C (less than 6 μm in total) with Pt clinical electrodes as comparison. They found that the PEDOT:PSS microelectrodes exhibited ten times lower impedances than Pt microelectrodes, and showed the first PEDOT:PSS recorded stimulus-locked human cognitive activity with changes in amplitude across pial surface distances as small as 400 μm.

In addition to the improvement of electrochemical characteristics such as impedance, there are also many studies devoted to improving the physical properties of devices. The transmittance is another important direction for flexible electrodes besides high-density. Higher transmittance can improve the optical imaging effect with a clearer spectral imaging map. Besides, transparent electrodes are suitable to be combined with light stimulation modules for the bidirectional interaction with brain, and help reduce photoelectric artifacts in the recording signals induced by the light. A gold nanonetwork (Au NN)-based transparent neural electrocorticogram (ECoG) monitoring system was proposed in implantable neural electronics (Figure 2c) [85]. By using the Au NN, the transmittance of microelectrodes increased by 81%, and furthermore a low electrochemical impedance of 33.9 kΩ at 1 kHz with improved mechanical stability was achieved. Polymer nanofibers were prepared on gold film, polymethylmethacrylate (PMMA) nanofibers were used as template, and the density of Au-NN was adjusted by controlling the electrospinning time. The density of nanofibers used for patterning the Au microelectrodes is a critical design parameter that determines electrical and optical properties.

The commercialization of the brain-computer interface has been widely valued. However, it is necessary to consider the balance of device cost and performance. A low-cost, multiplexed integrated μECoG system based on commercial electronics and flexible printed circuit board (flex-PCB) manufacturing has been developed, with a flexible printed circuit board that can meet the needs of mass production [89]. The electrode array has 61 contacts with a diameter of 203 μm, a spacing of 406 μm and a total thickness of about 30 μm. By multiplexing, the device successfully reduced the number of electrode wires and the PCB was made of cheap manufacturing and assembly specifications. The costs of the μECoG electrode array and the headstage can be controlled at about $29 and $130 (US Dollar), respectively.

Most flexible electrodes for the spatiotemporal mapping of neural interactions still need extensive craniotomy, which may affect brain function and cause irreversible damage. In order to reduce the craniotomy area, a flexible microelectrode device named iWEBS (insertable wrapping electrode array beneath the skull) was proposed, which could be inserted through a small cranial suture and wrapped stably on the cortical surface of living mice to minimize brain injury (Figure 2d) [56]. A slit with a size of merely 0.7 mm × 2.5 mm was opened in each hemisphere of the brain. The inserted electrodes were firmly pressed in place by the skull, which facilitated chronic and stable recordings in freely moving animals without the need for additional adhesive materials. In addition, they adopted a bifurcated flap shape, which enabled robust penetration and attachment to both hemispheres without damaging the blood vessels located at the midline (superior sagittal sinus) of the brain. Resection of a large area of the skull can easily lead to edema and deformation of the brain, which may lead to serious dislocation of the target area of cerebral cortex and affect the accuracy of detection.

2.1.2. Soft Planar Structure

Although a flexible structure can adapt to uneven surfaces, its mechanical mismatch with soft tissue is still challenging as a long-term stable interface. Thin-film electrodes with high stretchability are more adapted to the cortex surface with folds and wrinkles.

However, the common materials and fabrication processes have severely restricted the soft electrodes able to combine high electrode density and long-term stability. The development of soft material and stretchable neural implantation devices combined with planar layout have thus been an aspect worthy of attention. They can adapt to a small range of rugged surfaces and achieve a close fit with the cerebral cortex, which is conducive to the fixation of devices and the acquisition of clear neural signals. Here, Klas et al. developed a soft, high-density, stretchable electrode grid (SEG) based on an inert, high-performance composite material comprising gold-coated titanium dioxide nanowires embedded in a silicone matrix (Figure 2e) [72]. Gold-coated titanium dioxide nanowires have good conductivity, satisfactory electromechanical property and long-term stability. High-density SEG with a thickness of about 80 μm and 8 × 4 electrodes sites of 50 μm × 50 μm in size was obtained by using a filter lithography mask and dry etching. It enabled the device to record high spatiotemporal signals in freely moving rats for three months and minimized the craniotomy size for low invasiveness.

Some other researchers also choose soft, stretchable materials in planar ECoG electrodes to conform the brain tissue. For example, a PDMS-based soft, stretchable, 16-channel ECoG array was proposed with gold nanowire (Au NW) tracks and platinum (Pt) particle electrodes (Figure 2f) [86]. The electrode site was designed as a ring with an inner diameter of 200 μm and outer diameter of 400 μm with optical transparence, to be compatible with wide-field and 2-photon calcium imaging. Another way to balance the stretchability and traditional fabrication processes is the structure design, such as the serpentine conductive leads embedded in polymer films attached to the soft elastic substrate (Figure 2g) [87]. To improve the adhesion strength, a layer of titanium/silicon dioxide (5/50 nm) was deposited on the back of serpentine structures. Then, the device was strongly covalently bonded to the silicone base with treatment of UV-ozone. This work provides a simple but adaptable method to apply the reliable stretchable electrodes either in vitro or in vivo.

2.2. Open-Mesh Layout

Of the diverse electrode layouts, an open-mesh on the flexible substrate is widely used to realize better conformability on the cerebral cortex or into the deep brain regions. Here, we will introduce four types of representatives with open-mesh layout: hole mesh, finger mesh, three-dimensional mesh, and kirigami mesh.

2.2.1. Hole Mesh

In 2010, Kim et al. proposed specialized square mesh designs and ultrathin forms for the polyimide-based electrodes (2.5 μm in total), which ensured minimal stresses on the tissue and highly conformal coverage, even for complex curvilinear surfaces, as confirmed by experimental and theoretical studies (Figure 3a) [74]. The key function is the silk material in it that will dissolve and reabsorb in the cerebral cortex environment, as well as a spontaneous and conformal wrapping process that begins under the driving of capillary force. Similar work was also presented by clinically-friendly silk-supported/delivered bioelectrodes with ultrathin polyimide substrate defined by the square hole mesh (Figure 3b) [90]. The silk is applied as the supporting substrate with its degradation product of amino acids, which will be totally absorbed in the body with no side effects. Spatiotemporal ECoG detecting/monitoring, electro-neurophysiological neural stimulating/decoding controllable loading/delivery of therapeutic molecules, and parallel optical readouts of operating states can also be realized for customizable intracranial applications.

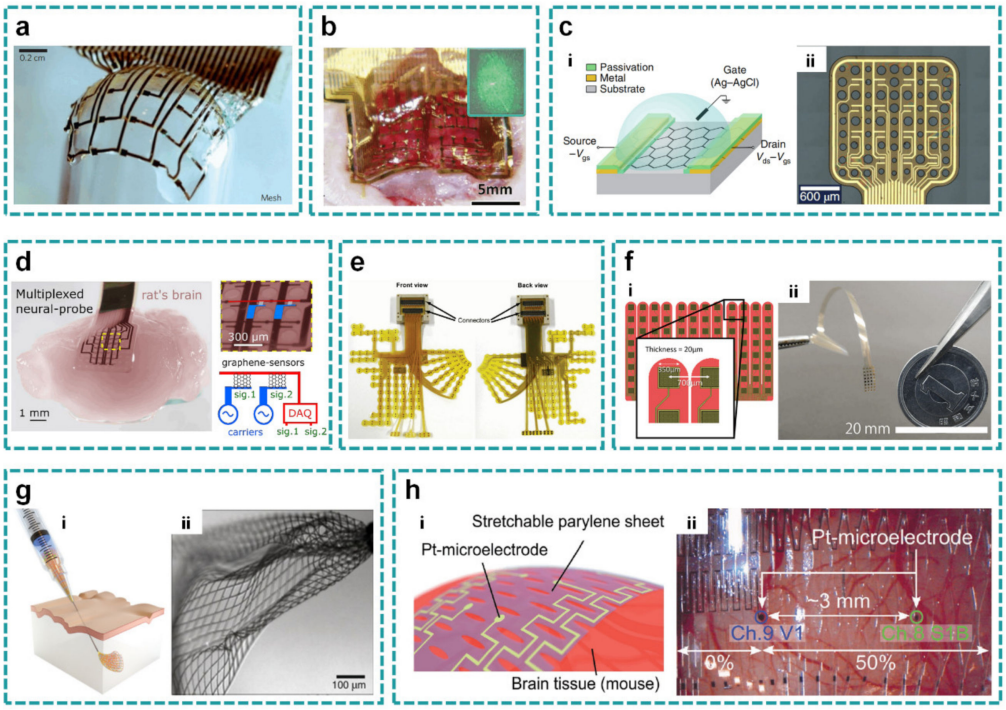

Figure 3. Open-mesh layout. (**a**) specialized square mesh designs and ultrathin forms for the polyimide-based electrodes (reprinted with permission from [74]); (**b**) clinically-friendly silk-supported bioelectrodes with ultrathin polyimide substrate structured by the square hole mesh (reprinted with permission from [90]); (**c**) flexible epicortical arrays of graphene solution-gated field-effect transistors (gSGFETs) on the polyimide substrate structured by the round hole mesh (reprinted with permission from [91]); (**d**) a multiplexed round-hole neural probe with frequency-division multiplexing of neural signals by graphene sensors (reprinted with permission from [92]); (**e**) a finger-like ECoG array to record neural activity simultaneously from different regions (reprinted with permission from [93]); (**f**) a finger-like 96-channel ECoG array with high temporal and spatial resolution (reprinted with permission from [94]); (**g**) the syringe injection of submicrometer-thick, centimeter-scale macroporous 3D mesh electrodes through needles (reprinted with permission from [73]); (**h**) A Pt microelectrode array embedded in 11 μm thick krigami parylene film (reprinted with permission from [95]).

The round hole mesh is another alternative for the flexible substrates to conformally couple with cortical surfaces. Eduard et al. used flexible epicortical arrays of graphene solution-gated field-effect transistors (gSGFETs) on the polyimide substrate with round holes of various sizes to map cortical spreading depression in rats (Figure 3c) [91]. They demonstrated that gSGFETs were able to record, with high fidelity, infralow signals (<0.1 Hz) to the typical local field potential bandwidth. In another work, Ramon et al. demonstrated the high performance of graphene transistors as mixers to perform amplitude modulation (AM) of neural signals in situ, which was used to transmit multiple signals through a shared communication channel (Figure 3d) [92]. Round holes with a diameter of 200 μm were distributed uniformly on the substrate to ensure better attachment. This kind of mesh layout has large coverage of the brain cortex with fine conformality, which can be extended to other flexible sensor designs.

2.2.2. Finger Mesh

The microelectrode array shaped by finger mesh can be accurately arranged in the specific regions of brain, while separating all channels in several individual groups on the finger mesh. Fukushima et al. developed a new ECoG array to record neural activity simultaneously from much of the medial and lateral cortical surface of the left hemisphere, together with the supratemporal plane (STP) of the lateral sulcus in macaque monkeys

(Figure 3e) [93]. The ECoG array consisted of 256 electrodes for bipolar recording at 128 sites. The "finger" electrode strips extended dorsoventrally or cau-dorostrally with four array compartments. Similarly, Kaiju et al. developed an ECoG array with high temporal and spatial resolution to decode the somatosensory evoked potentials (SEPs) (Figure 3f) [94]. The 96-channel array on a separated finger-like structure was mainly located in the finger representative area of the somatosensory cortex of rhesus monkeys and partially inserted into the central sulcus. The finger mesh structure separates the whole device into parts to further improve the conformality to the rugged brain surface, which inspires other kinds of flexible devices. However, the finger mesh structure is still not the best solution, as it restricts the distribution of electrodes in a local area.

2.2.3. Three-Dimensional Mesh

Most open-mesh electrodes are fabricated in 2D and used to cover the uneven cortical surface. Recently, 3D mesh electrodes are developed and injected into the deep brain regions. Except for the planar 2D mesh, the flexible electrodes with 3D mesh can be delivered into the internal brain regions. Jia et al. demonstrated the syringe injection (and subsequent unfolding) of submicrometer-thick, centimeter-scale macroporous mesh electronics through needles with a diameter as small as 100 μm (Figure 3g) [73]. In situ imaging and modelling showed that optimizing the transverse and longitudinal stiffness enabled the SU-8 based mesh to 'roll up' when passing through needle constrictions. The syringe-injectable electronics could serve as a unique yet general platform for building direct neuron–nanoelectronics interfaces for in-vivo studies. In another study, Xie et al. designed a three-dimensional macroporous nanoelectronic brain probe that combined ultra-flexibility and subcellular feature sizes to minimize mechanically induced scarring and allow interpenetration and integration of neurons [96]. The transverse compressive strain elements were incorporated to generate positive transverse curvature and yield a cylindrical global probe structure, and local tensile strain elements in the supporting arms of each sensor device were incorporated to produce negative curvature, bending the devices away from the surface of the cylinder. The ultra-flexible 3D macroporous probe could be stereotaxically implanted in a frozen state into rodent brains with minimal surgical and acute tissue damage. The co-existence of implanted devices and biological tissues is realized by the three-dimensional macroporous structural characteristics on the device, which significantly reduced tissue damage.

2.2.4. Kirigami Mesh

The open-mesh structure can be developed with stretchability to allow deformation with the soft brain. An ultrastretchable film device was realized by patterning slits as a Kirigami design (Figure 3h) [95]. A Pt/Ti-microelectrode array embedded in 11 μm thick parylene film with 5 × 91 slits exhibited a film strain of ≈250% at 9 mN strain-force (0.08 MPa in stress) with a Young's modulus of 23 kPa and maximum stretchability of 470%. Therefore, the Kirigami mesh design significantly reduces the film's strain-force compared to the conventional stretchable elastomer substrates. The Kirigami-based microelectrode device can simultaneously record in-vivo electrocorticogram signals from the visual and barrel cortices of a mouse by stretching the film and tuning the electrode gap. However, the Kirigami mesh may warp and deform vertically, which will adversely affect the adhesion between electrodes and cerebral cortex under large deformation. Therefore, how to eliminate the influence of out-of-plane deformation to the cerebral cortex is an urgent problem in the mesh of Kirigami design.

2.3. Probe Layout

Unlike the devices of planar layout and open-mesh layout which are applied on the cortex for ECoG signals, some electrodes need to be implanted into the deep brain, such as probes and microwires, which can detect and record the signal of specific smaller brain areas. The rigid Michigan probes are the most widely used penetrating devices to

interface with neurons. However, the serious mechanical property mismatch between rigid probe and brain tissue results in frequent neuroinflammation and scar formation. Furthermore, the generation of glial scars will seriously degrade the quality of neural signals. To solve these problems, flexible or soft polymers are applied as the substrates to replace conventional silicon probes.

In 2013, Tae-il et al. introduced an injectable class of cellular-scale optoelectronics that integrated multifunction components on the PET-based probe, with examples of unmatched operational modes in optogenetics, including completely wireless and programmed complex behavioral control over freely moving animals [18]. The whole probe structure is divided into four layers with a total thickness of ~20 μm, including a Pt microelectrode for electrophysiological recording or electrical stimulation, a micro inorganic photodetector based on ultra-thin silicon photodiode, a collection of four μ-ILEDs connected in parallel, and a precise temperature sensor or micro heater. The SU-8 based microneedle bonded to the bottom layer with a thin, bio-resorbable adhesive based on a film of purified silk fibroin, which enabled removal of the microneedle after implantation. Thus, this ultrathin, mechanically compliant, biocompatible device could afford minimally invasive operation in the soft tissues of the mammalian brain. Since the devices of probe layout can penetrate into the brain tissue, the multi-module integrated probe based on flexible substrate is different from the ECoG electrodes. It is a trend to control the neural circuits in the deep brain by the temperature, drugs, and optical stimulation with the multifunctional flexible probes.

For probes made of low stiffness materials, the commonly used implantation method is to use the rigid shuttle as a carrier to provide the probe with the required stiffness during implantation, and then withdraw the shuttle after the probe is implanted. Temporary shuttles have been developed with soluble supporting materials such as silk, sugar, hydrogel, etc. as coating, and metal as inserted rigid backbone layer [4,5,7,97]. Zhang et al. reported a simple but robust mobile insertion shuttle consisting of a steel needle with a dissolvable spheroid micropost for easier removal after probe implantation (Figure 4a) [97]. A simple dip-coating process was used to create the dissolvable spheroid PEG micropost on the insertion shuttle, which was based on the competition and balance between the gravity and surface tension. In this way, the ultraflexible PI-based neural probe was successfully implanted into the target brain region easily and quickly. The mechanical stiffness of the flexible probe can be further reduced by the structure design. Guo et al. introduced the paper-cutting Kirigami structure to the probe layout with low Young's modulus and excellent stretchability [98]. Meanwhile, the slits on the substrate allowed the electrode sites floating out of plane and the circulation of the cerebrospinal fluid which would further enhance biocompatibility. The probe tip was designed with a hole with a diameter of 0.5 mm, so the probe could be accurately implanted into the brain with the aid of a steel needle. However, although a series of subtle experiments have been done to obtain accurate control of PEG micropost to reduce the damage during implantation, the existence of the shuttle inevitably increases the damage to the brain during its insertion and withdrawal.

The most immediate way to develop devices with good softness is to choose materials with low Young's modulus, so as to reduce the damage to the brain as well as the foreign body reaction, which can cause local swelling and an inflammatory reaction. In a recent study, Gallium (Ga) was used inside of a probe structure with the adjustable rigidity by five orders of magnitude before and after the insertion to the brain, due to the solid-liquid phase change of liquid metal at body temperature and the consequent shape deformation of the probe. Thus, the probe could be delivered into the deep brain region without an external shuttle vector (Figure 4b) [81]. Pressurized liquid Ga was introduced into the stretchable microfluidic "hardening" channel to deform and expand the cross section of the probe, and then frozen to solid state to obtain a rigid probe for deep brain implantation. Once implanted, the probe would become soft and flexible in a few minutes. Miniaturized design and soft material PDMS were adopted to reduce the tissue damage caused by the probe moving in all directions. Another approach to obtain the soft neural probe is 3D printing. Hyunwoo et al. introduced a 3D printable conducting polymer ink based on the

poly(3,4-ethylenedioxythiophene):polystyrene sulfonate (PEDOT:PSS) with high performance, which could be integrated with insulating elastomers (PDMS) via multi-material 3D printing in a facile, fast, and significantly streamlined manner (Figure 4c) [77]. The multi-material 3D printing capability in high resolution allowed printing both insulating encapsulation (PDMS ink) and electrodes (conducting polymer ink) of the neural probe by a facile continuous printing process without the need of post-assemblies or complex multi-step procedures in conventional fabrication methods such as electron-beam lithography. The resultant probe consisted of nine PEDOT:PSS electrode channels in the feature size of 30 μm in diameter with the impedance in the range of 50–150 kΩ at 1 kHz, suitable for in-vivo recording of neural activities.

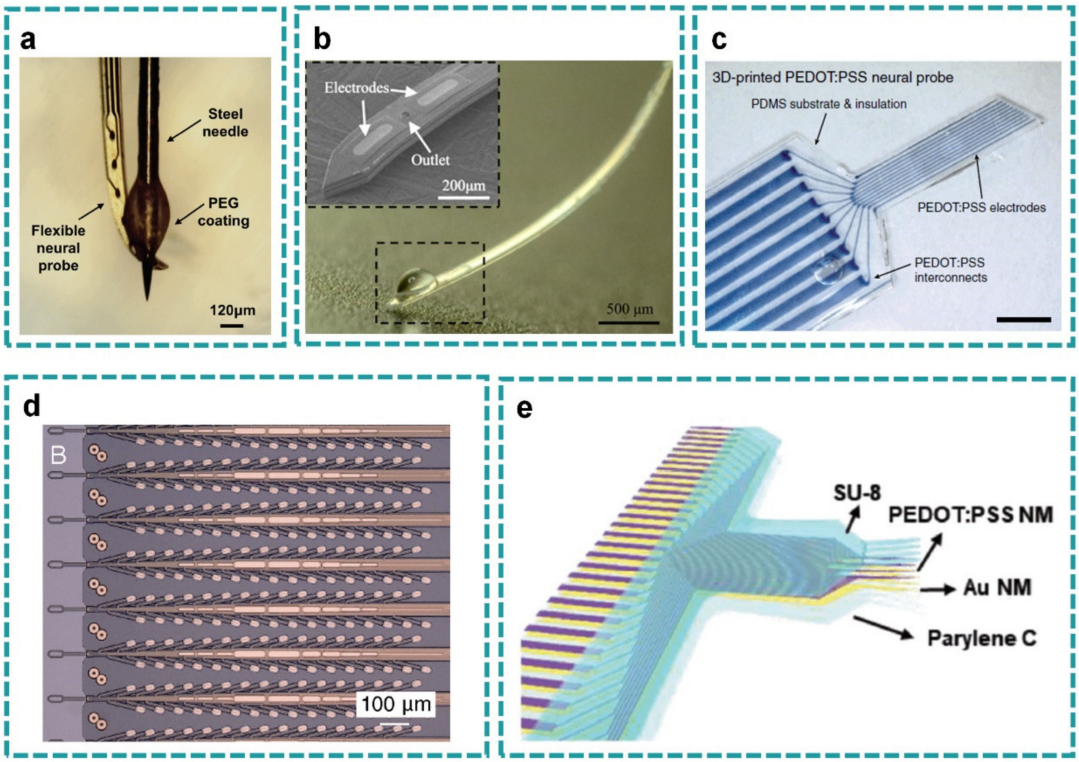

Figure 4. Probe layout. (**a**) a flexible neural probe with the simple but robust mobile insertion shuttle consisting of a steel needle with a dissolvable spheroid micropost (reprinted with permission from [97]); (**b**) the PDMS-based probe with embedded Gallium (Ga) could be adjusted by five orders of magnitude before and after the insertion into the targeted brain region (reprinted with permission from [81]); (**c**) a high-performance 3D printed probe fabricated by the printable conducting polymer ink; scale bar, 1mm (reprinted with permission from [77]); (**d**) the arrays of small and flexible electrode "threads" with up to 3072 electrodes (reprinted with permission from [49]); (**e**) a penetrating microelectrode probes in array focusing on light transmittance (reprinted with permission from [82]).

A single neural probe can only collect limited data at one local position, so the multi-shank probe array stands as a common solution to record more neural signals across multi-regions. Musk et al. contributed to the commercialization of BCI by developing a neurosurgical robot specially used for flexible neural probe implantation (Figure 4d) [49]. They built arrays of small and flexible electrode "threads", with up to 3072 electrodes distributed on 96 threads in each array. The neurosurgical robot was capable of inserting six threads per minute, that is, 192 electrodes. A large number of fine and flexible PI-based probes were effectively and independently inserted into multiple brain regions, and each wire could be inserted into the target region of the brain with micron accuracy, while avoiding surface blood vessels. The system achieved a peak yield of up to 70% in long-term implantation electrodes. Zhao et al. proposed a kind of multi-shank ultraflexible neural electrode array with surgical footprints as small as 200 μm^2 to conduct minimally invasive

experiments in a mouse model [75]. The alignment of probes was guided by making microprism on the reticular substrate, and the electrode array was implanted into the cerebral cortex by using arrays of tungsten microwires as shuttle devices and bioabsorbable adhesive polyethylene glycol (PEG) to temporarily attach a shank onto each microwire. The smallest inter-shank spacing they demonstrated using the microtrenches guided microwire arrays was 150 μm, which was comparable to the closest spaced silicon neural probes and Utah arrays. PEG coating will dissolve in the brain tissue environment in less than 2 min, thus the insertion time is limited. For probe electrodes, the fabrication of shuttle and surface coating needs to be controlled precisely, which can not only assist probe implantation, but also minimize damage. This requires the choice of proper materials for shuttle and coating, as well as precise size control.

Kyung et al. designed a penetrating microelectrode array focusing on light transmittance (Figure 4e) [82]. They used polyethylene glycol to temporarily harden the nanonet array, thus inserted the probe into the brain in a minimally invasive environment. The array has good robustness in 1000 bending cycles and high transmittance of 67% at 550 nm, which is suitable for the combination of various optical methods. In another study, a biodegradable shuttle structure was added to assist penetration of the flexible probe array [53]. Wang et al. designed a parylene C polymer neural probe array with 64 microelectrodes across 8 individual shanks to anatomically match specific regions of the hippocampus of rats. It is worth noting that the mechanical support technology developed in this work involves a new type of biodegradable polymer scaffold, which can temporarily shorten the shank length and thus increase its stiffness during implantation. Therefore, it enables access to deeper brain regions while preserving a low original cross-sectional area of the shanks. A single shank of probe can only record the neurons in a small region. Therefore, the probe array with multi-shanks should be developed to satisfy the necessity of multi-region acquiring as well as stimulation.

2.4. Micro-Wire Layout

Flexible micro-wire layout is a common strategy to acquire signals or electrical stimulation to the target brain regions. Zhao et al. proposed a graphene encapsulated copper (G-Cu) microelectrode to avoid the toxicity of copper for direct implantation (Figure 5a) [41]. Graphene encapsulation layer was directly deposited on the surface of copper microfilament by low-pressure chemical vapor deposition, providing a seamless and fully covered graphene coating and an impermeable barrier to copper corrosion. Besides, the G-Cu microelectrodes show no image artifacts in a 7.0 T MRI (magnetic resonance imaging) scanner, indicating minimal magnetic field distortion in their vicinity. This high MRI compatibility (which should have no image artifacts and get minimal magnetic field distortion in its vicinity) can create new opportunities for fundamental brain activity studies and clinical applications requiring continuous MRI and electrophysiological recordings.

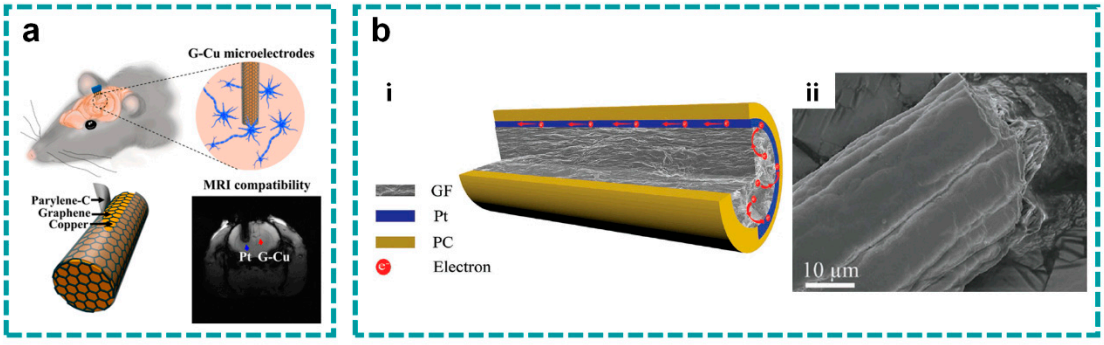

Figure 5. *Cont.*

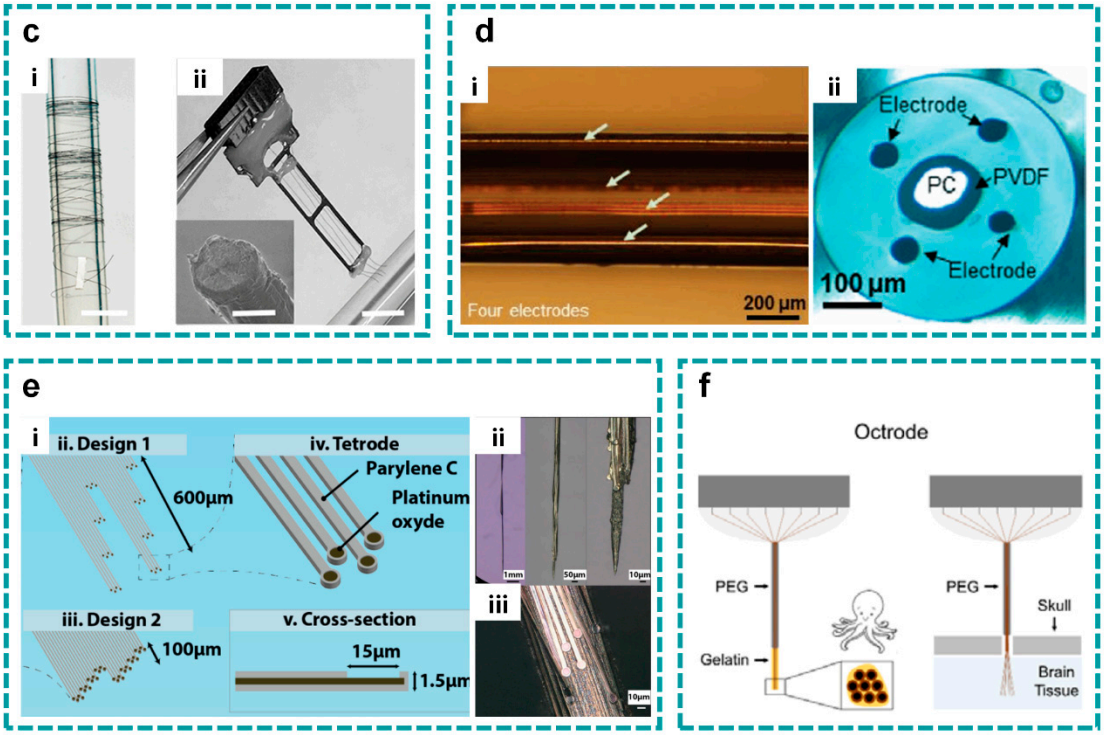

Figure 5. Micro-wire layout. (**a**) a graphene encapsulated copper (G-Cu) microwire electrode to avoid the toxicity of copper for direct implantation (reprinted with permission from [41]); (**b**) graphene microwires with unique mechanical and electrochemical properties (reprinted with permission from [76]); (**c**) a soft and MRI compatible implantable microwire electrode based on the carbon nanotube fibers; i: scale bar, 5 mm; ii: scale bar, 5 mm. Inset, SEM image of a CNT fiber electrode tip; scale bar, 10 µm (reprinted with permission from [99]); (**d**) a composite flexible multimode microwire probe composed of metal electrodes and double-clad waveguides (reprinted with permission from [100]); (**e**) NeuroRoots as microwire layout with similar dimension to neurons, mechanical flexibility and spatial distribution (reprinted with permission from [83]); (**f**) the self-expanding octopus-like microwire electrode array (reprinted with permission from [101]).

Carbon-based micro-wires have been more popular recently, compared to metal microwires, for their better biocompatibility and good mechanical and electrochemical properties. Graphene microwires developed by Wang et al. not only possessed natural biocompatibility, but also kept unique mechanical and electrochemical properties (Figure 5b) [76]. By applying a thin platinum coating on wet-spun graphene microwires as a current collector, the resistivity of graphene fibers was reduced. The electrochemical properties of graphene and the electronic properties of Pt were combined with microelectrodes, without limiting its mechanical flexibility and high surface area. The low impedance and porous structure of graphene microwires can provide a high charge injection capacity and record and detect neuronal activity in a much smaller area than the prior methods. In another work, Lu et al. developed a soft and MRI compatible implantable electrode for use in chronic longitudinal studies employing both MRI and electrophysiology (Figure 5c) [99]. The diameter of carbon nanotube fibers ranges from 20 to 5 µm and its bending stiffness is one order of magnitude smaller than the previously reported microwires. Under the 7.0 T magnetic resonance scanner, the carbon nanotube microwire electrode shows excellent interface electrochemical performance and greatly reduces magnetic resonance imaging artifacts. Using a shuttle-assisted implantation strategy, soft carbon nanotube microwire electrodes can accurately target specific brain regions and record high-quality single-unit neural signals. Besides, the brain inflammatory responses are greatly reduced compared with their stiff metal counterparts. Although their service life is shorter than some flexible polymer electrodes, their active sites with 5 microns in diameter significantly improve the stimulation resolution and facilitate the identification of individual neurons in record-

ing. They are expected to be developed as the new high-density intracellular probes with thousands of channels in the future.

The multifunctional micro-wire electrode is an emerging direction by introducing the waveguides or microfluidic channels. Du et al. designed a composite flexible multimode microwire probe composed of metal electrodes for recording neural signals and double-clad waveguides for optical stimulation (Figure 5d) [100]. To improve the optical transmission performance, the double-clad waveguide is used to confine the light to the inner core, and the metal electrode is embedded in the outer layer of the optical microwire probe. This configuration makes the optical microwire probe acquire more than 90% excellent optical transmission performance, high flexibility and mechanical properties, and low specific impedance. In addition, the functional optical fiber probe can be produced by hot stretching technology with low cost and high yield.

When the flexible polymer-based electrodes are thin and narrow enough, they could be implanted into the deep tissue like microwires. Ferro et al. designed and created NeuroRoots, a bio-mimetic multi-channel implant sharing similar dimension (10 μm wide, 1.5 μm thick), mechanical flexibility and spatial distribution as axon bundles in the brain, yet centimeters long, organized in axon-like tendrils (Figure 5e) [83]. Each electrode is independent, allowing complete flexibility in the number of electrodes at a given depth, without increasing the electrode width, and thus damage. NeuroRoots electrodes detected action potentials reliably for at least 7 weeks in rats and the signal amplitude and shape remained relatively constant during long-term implantation. Guan et al. also developed a similar implant named Neurotassel, consisting of an array of flexible and high–aspect ratio microelectrode filaments up to 1024 channels, each with a neurite-scale cross-sectional footprint of 3 μm × 1.5 μm, to form implantable fibers with a total diameter of ~100 μm [64]. Another similar electrode array is the self-expanding octopus electrode array, which could effectively minimize the hardness of the implant and the damage to the tissue near the recording site (Figure 5f) [101]. The octrode array was fabricated by enwrapping a bundle of eight formvar-coated nickel-chromium microwires with a layer of polyethylene glycol in a custom-made mold. After the electrodeposition of platinum nanoparticles, the microwires at the electrode tip were gathered together and then re-enwrapped with a thin layer of gelatin to maintain their structure and mechanical strength for implantation. The biocompatible gelatin coating expanded and dissolved rapidly, and the collected microwires self-spread at the implantation site, thus adhering to the cerebral cortex.

3. Fabrications

3.1. High Resolution

Photolithography is the common fabrication approach to realize high-resolution, which refers to the technology of transferring the pattern on the mask to the substrate by means of photoresist under the action of light. The NeuroGrid designed by Dion et al. has an electrode surface area of only 10 μm × 10 μm and an interelectrode spacing of 30 μm (Figure 6a) [68]. These ultrasmall microelectrodes on the NeuroGrid can record both local field potentials (LFPs) and action potentials from superficial cortical neurons without penetrating the brain surface, both in behaving rats and in human patients undergoing surgery to treat epilepsy. Thanks to the reliable photolithography, the scalable, neuron-sized-density electrodes allow isolation and characterization of multiple individual neurons′ action potential waveforms across the cortical surface. In another study, Yang et al. designed a Si shadow mask combined with electron beam evaporation and chemical vapor deposition technology (Figure 6b) [78]. The deposited chromium/gold layer was patterned by the shadow mask, which was obtained from the traditional photolithography process. This method guaranteed that the line-width of gold electrode reached 5–100 μm.

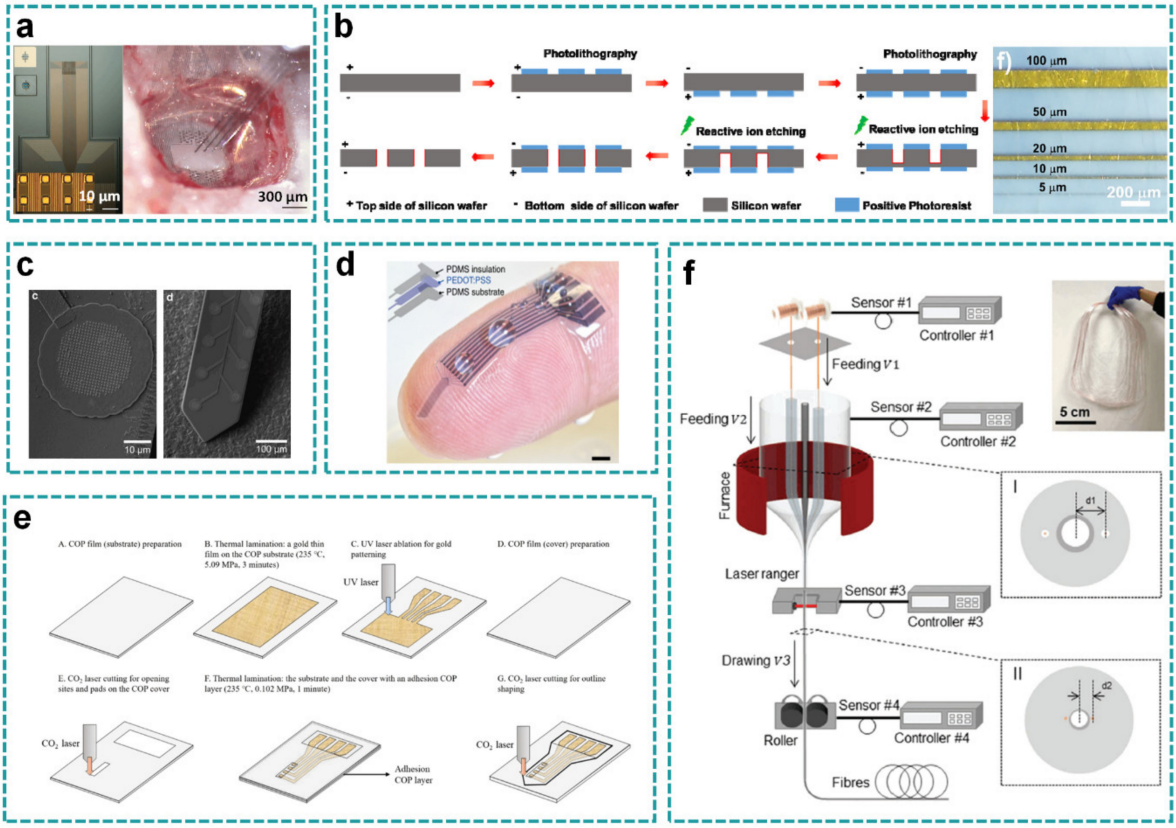

Figure 6. High resolution. (**a**) the NeuroGrid fabricated with conventional photolithography has an electrode Scheme 10 μm × 10 μm and an interelectrode spacing of 30 μm (reprinted with permission from [68]); (**b**) a Si shadow mask combined with electron beam evaporation and chemical vapor deposition technology (reprinted with permission from [78]); (**c**) a polymer probe with 32 recording sites by an improved electron beam lithography (EBL) process of polymer substrate (reprinted with permission from [102]); (**d**) a simple CO_2 laser machining process of a neural probe based on the cyclic olefin polymer (COP); scale bar, 1 mm (reprinted with permission from [103]); (**e**) 3D printable conducting polymer ink based on poly(3,4-ethylenedioxythiophene):polystyrene sulfonate (PEDOT:PSS) for 3D printing of conducting polymers as neural probe (reprinted with permission from [77]); (**f**) the composite flexible multimode optical fiber probe fabricated by a strategy of compound scaling and shrinking process (reprinted with permission from [99]).

New methods are also developing to realize high resolution, including electron beam lithography (EBL), laser micromachining, 3D printing, thermal drawing, etc. Electron beam exposure is a technology that uses electron beams to directly draw or project and copy graphics on a wafer coated with photoresist. It has the characteristics of high resolution (the limit resolution can reach 3~8 μm), easy generation and modification of graphics, and a short production cycle. Laser micromachining can produce a smooth cutting surface without causing surrounding deformation, and its machining accuracy can reach 10 μm. At present, 3D printing and thermal drawing has only been tried on individual devices, and its process effects and indicators still need to be clarified and improved. EBL technology can realize high pattern resolution and ensure good alignment accuracy. However, because the insulating surface will cause an unnecessary charging effect in the exposure process, and the beam itself and the processing required to construct the EBL resist mask may damage the polymer film, it is difficult to carry out EBL for polymer substrate. Kee Scholten and Ellis Meng developed an improved EBL process for polymer substrate and designed a polymer probe with 32 recording sites patterned along a 2 mm long Parylene-based shank and critical dimensions as small as 250 nm (Figure 6c) [102]. Submicron structures, including conducting traces, serpentine resistors, and nano-patterned electrodes, were machined and presented as components in robust, flexible, free-film devices. The EBL with

smaller feature size removes the limitation on recording density of polymer neural probes, with mechanical and material properties better suited for chronic implantation than silicon.

For the flexible probe fabricated by 3D printing technology, its unique advantages of programmability, facility, and high throughput are unmatched by conventional methods, and the processing of microscale patterns is not inferior to inkjet printing and screen printing. Hyunwoo et al. introduced a high-performance 3D printable conducting polymer ink based on poly(3,4-ethylenedioxythiophene):polystyrene sulfonate (PEDOT:PSS) for 3D printing of conducting polymers (Figure 6e) [77]. Its special PEDOT:PSS ink can change the size of electrodes by changing the size of nozzle. The resulting conductive polymer ink shows excellent 3D printability, which can be produced with high resolution (over 30 μm), high aspect ratio (over 20 layers) and highly reproducible conductive polymer, and it is also easy to integrate with other 3D printable materials such as insulating elastomers through multi-material 3D printing. The printed probe consists of nine PEDOT:PSS electrode channels in the feature size of 30 μm in diameter with the impedance in the range of 50–150 kΩ at 1 kHz, suitable for in vivo recording of neural activities. However, although this approach has achieved relatively high printing accuracy, it is still not ideal compared to traditional photolithography or some other new methods. Besides, the printing materials are limited. For some composite materials, maintaining a high accuracy is difficult. Thanks to the convenience and batch processing ability of 3D printing, it can rapidly structure the flexible thin film devices with unconventional materials, such as conductive polymers.

In addition to 3D printing, some other processes are also successfully applied to obtain the high-resolution electrodes instead of the mask patterning, which simplify the process to some extent. Shinyong et al. developed a simple laser machining process of a neural probe based on the cyclic olefin polymer (COP) (Figure 6d) [103]. Due to the good adhesion to gold, the gold film can be thermally laminated on the COP substrate using a heating press without an adhesive layer. The gold thin film can be micromachined by ultraviolet laser ablation without damaging the copper substrate, because the COP substrate has ultraviolet transparency. Compared with metal deposition and photolithography techniques used to fabricate conventional polymer-based neural probes, this fabrication approach does not need masks, vacuum and fabrication facilities. They fabricated a COP-based depth neural probe with shank length of 10 mm, which was partially cut by a CO_2 laser with a wavelength of 10 μm. The electrode sites and connection pads were also opened by CO_2 laser cutting.

The composite flexible multimode optical fiber probe proposed by Du et al. was composed of a metal electrode for recording neural signals and a double-clad waveguide for optical stimulation (Figure 6f) [100]. Its metal electrodes are regularly embedded into biocompatible polymer fibers with double-clad optical waveguides by hot stretching. They put forward a strategy of compound scaling and shrinking process, which requires that the size of fibers remain unchanged or change continuously during drawing. The fabricated multimodal fiber probe is highly flexible with diameter of ~300 μm.

3.2. Special Substrates

For flexible thin-film devices, PI, Parylene, PDMS and the like are commonly used as substrate materials. They have lower Young′s modulus, which improves the matching degree between the device and the brain to some extent. However, these traditional materials lack some of the unique characters for specific applications, such as low permeability and poor water solubility, which affect the local tissue fluid flow to a certain extent, may cause rejection of organisms, and are not conducive to the specific demand of implantation in vivo. Substrates made of unusual materials show excellent properties. For example, Guo et al. designed a flexible neural electrode array based on hot-pressed nanopaper substrate (Figure 7a) [104]. Hot-pressed nanopaper has higher biocompatibility because of its good hydrophilicity and water wettability. Besides, nanopaper exhibits high flexibility and good shape stability. Dried and bleached pine wood pulp board in NaBr/NaClO/TEMPO solution was suspended to selectively oxidize hydroxymethyl

groups of cellulose fibers into carboxyl groups, so that oxidized fibers were decomposed into nano-cellulose fibers. The dispersion of nano-cellulose fibers was then filtered through nitrocellulose membrane to obtain wet gel membrane, and finally hot-pressed into nanopaper membrane at 120 °C and 15 kPa. The diameter of nano cellulose fiber is much smaller than the wavelength of light, which effectively reduces light scattering. The transmittance of hot-pressed nanopaper reached 96%. The neural electrode array based on nanopaper was released from the SiO_2/Si substrate and transferred onto a 40 μm-thick nanopaper substrate by a polymethylmethacrylate (PMMA)-assisted transfer technique.

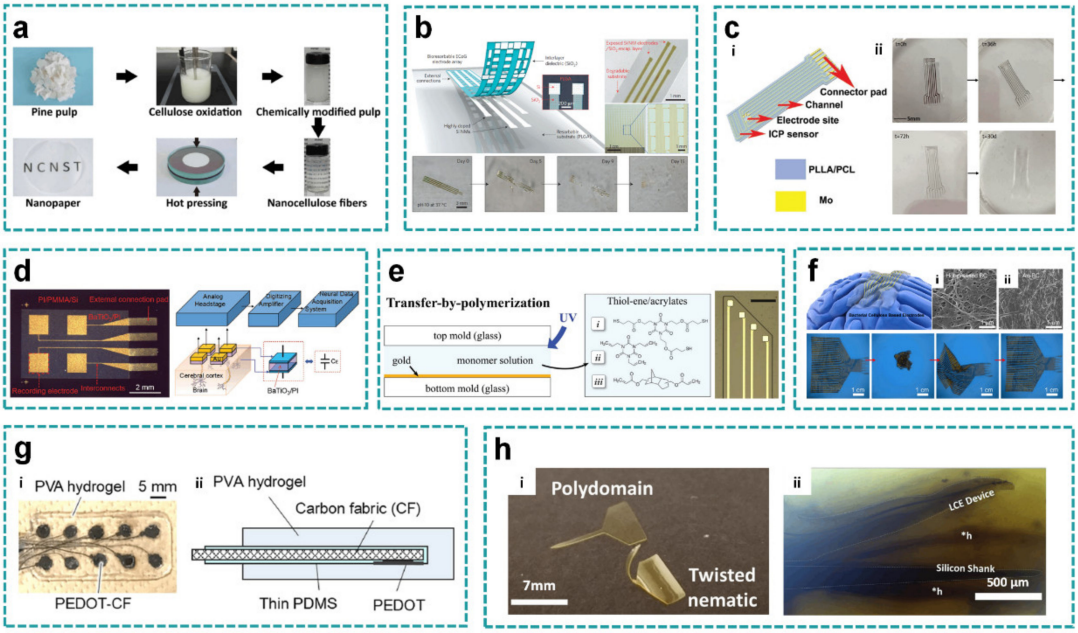

Figure 7. Special substrates. (**a**) a flexible neural electrode array based on hot-pressed nanopaper substrate (reprinted with permission from [104]); (**b**) a passive, bioresorbable neural electrode array using a film of SiO_2 and a foil of poly(lactic-co-glycolic acid) (PLGA) for ECoG and subdermal EEG measurements (reprinted with permission from [79]); (**c**) a bioabsorbable ECoG device using poly(l-lactide) (PLLA) and polycaprolactone (PCL) composite which can degrade slowly in biological fluid until it disappears completely (reprinted with permission from [105]); (**d**) the capacitive $BaTiO_3$/PI electrode array (reprinted with permission from [106]); (**e**) softening substrates for neural recording electrodes with the ternary thiol-ene/acrylate shape memory polymer networks (scale bar, 60 μm; reprinted with permission from [107]); (**f**) supersoft multichannel electrodes by depositing gold layers on thin bacterial cellulose (reprinted with permission from [78]); (**g**) a totally soft organic subdural electrode by hydrogel substrate (reprinted with permission from [108]); (**h**) LCE-based deployable intracortical microelectrode arrays (MEAs) (scale bar, 7mm in left and 500 μm in right; reprinted with permission from [109]).

Biodegradable materials are also applied for brain-computer interfaces as the substrates. These materials will dissolve gradually after being implanted for a certain period, thus reducing foreign body reaction or the need of a secondary operation. Yu et al. proposed the passive, bioresorbable neural electrode array for ECoG and subdermal EEG measurements. A photolithographically patterned, n-doped Si NM (~300 nm thick) defines the electrodes and interconnects. A film of SiO_2 (~100 nm thick) and a foil of poly(lactic-co-glycolic acid) (PLGA) (~30 μm thick) serve as a bioresorbable encapsulating layer and substrate, respectively (Figure 7b) [79]. It can be estimated that the present device designs and material choices allow complete dissolution of the device in two months. The flexible biodegradable devices can also be used to treat brain disorders where transient monitoring and modulation of physiologic function, implant integrity, and tissue recovery or regeneration are required. Xu et al. designed a bioabsorbable ECoG device integrated with an intracortical pressure sensor for monitoring swelling of the cortex during operation (Figure 7c) [105]. The substrate of the device is made of bioabsorbable material with poly(l-

lactide) (PLLA) and polycaprolactone (PCL) composite and transient metal molybdenum, which can degrade slowly in biological fluid until it disappears completely, thus avoiding the possible infection risk caused by electrode removal surgery. The biodegradable materials could not only used for transient BCI devices, but could also inspire the development of other implantable biosensors and actuators.

The capacitive-type electrodes can enhance safety by eliminating leakage currents between the devices and the biology, and also avoid irritation and allergic reactions that are caused by direct contact of metal electrodes. Chen et al. developed a barium titanate/polyimide ($BaTiO_3$/PI) nanocomposite with high dielectric constant, which was successfully synthesized and employed as the ultrathin dielectric layer of the capacitive $BaTiO_3$/PI electrode array (Figure 7d) [106]. For the sample with $BaTiO_3$ content of 40 wt.%, the dielectric constant was determined to be in the range of 30.14–51.54. Compared with the pure polyimide, the dielectric constant of the composite was obviously improved by 10–17 times. The capacitive $BaTiO_3$/PI electrode array can significantly attenuate the electrical leakage current during signal acquisition and ensure electrical safety for applications on surfaces of internal organs such as heart and brain. The signal quality of the prepared capacitive $BaTiO_3$/PI was equivalent to the obtained signals from the resistive electrode array, which can be used to manufacture the small-area capacitive coupling electrode arrays.

The application of several different chemicals to synthesize softening polymers and use them as substrate to improve biocompatibility has also been proposed [110–112]. Taylor et al. used the ternary thiol-ene/acrylate shape memory polymer networks to create softening substrates for neural recording electrodes (Figure 7e) [107]. The electrode was manufactured by photolithography and other traditional approaches. It can soften from more than 1 GPa to 18 MPa after implantation to reduce the mechanical mismatch at the biological-non-biological interface. Control of the glass transition temperature and modulus in physiological conditions was achieved by changing diacrylate content from 0 mol.% to 31 mol.%.

Bacterial cellulose, hydrogel, and liquid crystal polymer are also recently reported as the special soft substrates besides the shape memory polymer. Yang et al. presented supersoft multichannel electrodes by depositing gold layers on thin bacterial cellulose (BC) (Au-BC electrodes) (Figure 7f) [78]. The Young's modulus of BC substrate is 120 kPa, which can match well with the cerebral cortex, and thus improve biocompatibility. After the bacterial cellulose was harvested, the ultra-thin BC film was prepared by hot pressing. The absorbed water was removed by hot press until BC film became completely dry and smooth. By the electron beam evaporation, the pattern of chromium/gold layer was deposited on the substrate through shadow mask. Compared with the common polymer-based electrodes, the BC electrode exhibited excellent resistance to torsion and fatigue damage. Shuntaro et al. developed a totally soft organic subdural electrode by embedding an array of poly(3,4-ethylenedioxythiophene)-modified carbon fabric (PEDOT-CF) into the polyvinyl alcohol (PVA) hydrogel substrate (Figure 7g) [108]. Carbon fabric was cut into circular electrodes, its round back surface and wires were then insulated by coating thin PDMS, followed by electro polymerization of PEDOT on the exposed front surface of the carbon fiber round part. In the gelation process, the carbon fiber array was embedded in the hydrogel matrix. Compared with metal electrodes, carbon fiber has relatively lower magnetic susceptibility and higher resistivity, which reduces the risk of image artifacts and heat in the process of magnetic resonance imaging, and obtains better impedance characteristics through modification. As a matrix material, hydrogel can obtain mechanical properties close to biological tissues, excellent maneuverability, adhesion to brain surface, and permeability to body fluids.

The foreign body response (FBR) is a limitation for the chronic functionality of neural electrodes [2,7]. Liquid crystal elastomers (LCEs) are responsive materials capable of programmable and reversible shape change. These hydrophobic materials are also non-cytotoxic and compatible with photolithography, especially suitable as the substrate to minimize FBR. Rihani et al. explored the feasibility of LCE-based deployable intracortical

microelectrode arrays (MEAs) (Figure 7h) [109]. Liquid crystal molecules in LCEs show reversible shape changes when stimulated by temperature and light, and have biocompatibility in vitro. During processing, the LCE probe was released from the substrate and bent into a three-dimensional shape, so polyethylene glycol (PEG) was used to flatten the device. The PEG layer dissolved in physiological conditions, allowing the LCE probe to deploy post-implantation. LCE-based deployable intracortical MEAs were capable of maintaining electrochemical stability, recording extracellular signals from cortical neurons in vivo, and deploying recording sites greater than 100 μm from the insertion site in vivo.

In the past decade, the development of new materials has facilitated the fabrication of flexible thin film devices based on the special substrates. In the future, we can expect that more and more new materials with special properties will be used as the flexible substrates, including but not limited to: transparence, biodegradability, softness, and resistance.

3.3. Special Interconnects

The novel fabrication approaches of conductive interconnects in thin-film devices are also important according to the applications. Traditional precious metals like gold or platinum can be replaced by the emerging conductive materials as well as the corresponding fabrication methods.

Carbon-based materials, like carbon nanotubes, graphene, or carbon fibers, can be used as interconnects owing to their high flexibility and transparence, good electrical conductivity, and mechanical properties, relatively stable chemical properties, and good electrochemical properties. Dong-Wook et al. proposed a transparent micro-ECoG array based on graphene, which could be implanted on the brain surface of rodents for high-resolution neurophysiological recording (Figure 8a) [80]. Graphene has excellent electrical conductivity, thermal conductivity, transferability, strength, and adjustable electronic characteristics. The electrode sites and portions of the traces that were to be in contact with the brain were left for the subsequent graphene transfer and patterning, such that the brain contact area of the electrode would be transparent. Following metallization, four graphene monolayers were transferred and stacked sequentially onto the wafer surface, using the wet transfer technique. In addition, the photoelectric artifact is a serious issue to be avoided during optical stimulation due to the ionic charge transfer layer at the conductor-electrolyte interface. Photoelectric artifact refers to the large signal interference when the light source is turned on or off, so as to drown the original neural signal changes to be observed. Graphene exhibits relatively high work function and reduces photoelectric artifacts for its zero bandgap characteristics similar to metals.

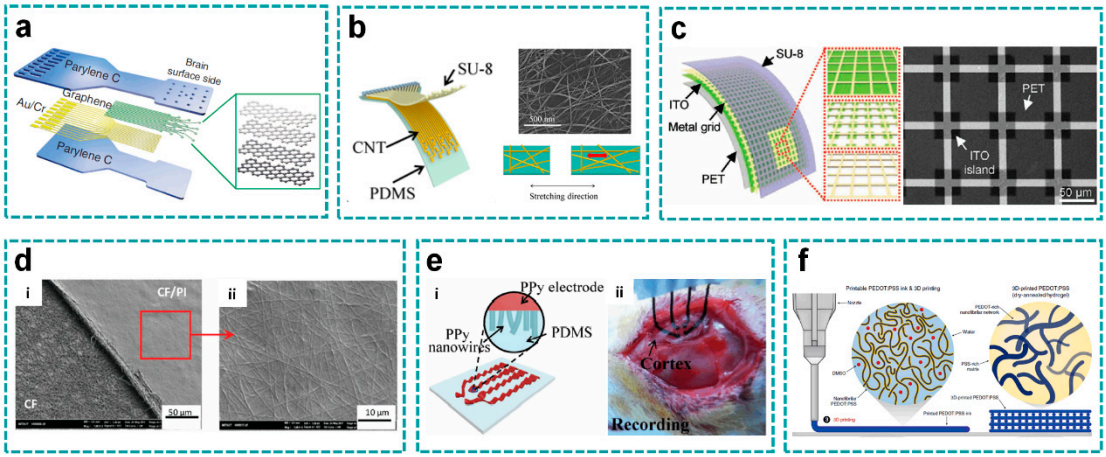

Figure 8. *Cont.*

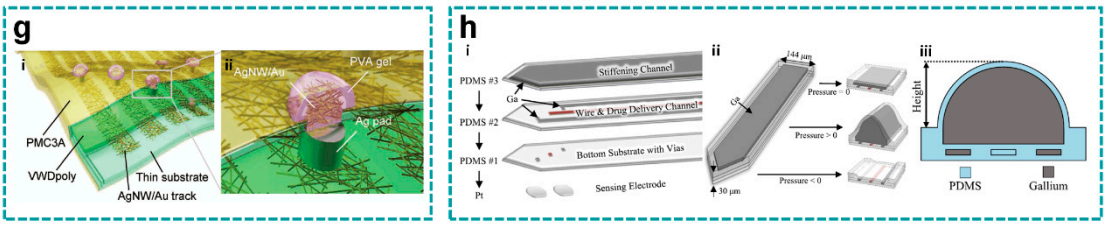

Figure 8. Special interconnects. (**a**) a transparent micro-ECoG array based on graphene (reprinted with permission from [80]); (**b**) a stretchable transparent electrode array from carbon nanotube (CNT) web-like Table [113]); (**c**) a high-performance indium tin oxide (ITO)/metal grid hybrid flexible transparent microelectrode (reprinted with permission from [114]); (**d**) a microfabrication technique for patterning flexible, cloth-like, polymer-derived carbon fiber mats embedded in polyimide (PI) by selective reactive ion etching (reprinted with permission from [115]); (**e**) polypyrrole (PPy) electrode materials modified by nanowires through a simple electro-polymerization process (reprinted with permission from [116]); (**f**) a novel 3D printable conducting polymer ink (reprinted with permission from [77]); (**g**) stretchable transparent Ag/Au nanowires encapsulated in transparent polymer and connected to hydrogel-coated microelectrodes through silver pads (reprinted with permission from [117]); (**h**) a neural probe using gallium (Ga) in the probe construction as interconnects (reprinted with permission from [81]).

Carbon nanotube can also be used as an interconnect thanks to its transparence and stretchability. Zhang et al. reported a stretchable transparent electrode array from carbon nanotube (CNT) web-like thin films that retained excellent electrochemical performance and broadband optical transparency under stretching, and were highly durable under cyclic stretching deformation (Figure 8b) [113]. When stretched to 20% strain, the carbon nanotube /PDMS composite kept high optical transparency, ensuring its reliable application with external deformation. By using different deposition parameters to change the film thickness, the transmittance and conductivity of carbon nanotube films can be adjusted. Thicker films have higher conductivity but lower optical transparency. The manufacturing process of the carbon nanotube stretchable transparent electrode array includes patterning the carbon nanotube film and the SU-8 insulating layer on the sacrificial substrate, and then coating the PDMS film on the carbon nanotube/SU-8 composite followed by removing the sacrificial substrate. In this way, the electrode array finally obtained does not contain opaque metal and shows high optical transparency. Meanwhile, the CNT electrodes show lower impedance than graphene electrodes. Under synchronous light stimulation/imaging, electrical recording can be performed with negligible light-induced artifacts, and real-time continuous recording can be performed under traumatic brain injury. This can help the study of optical imaging of the brain.

In another study, electrodes made by (ITO)/metal grid also had high transparency. Chen et al. developed a high-performance indium tin oxide (ITO)/metal grid hybrid flexible transparent microelectrode with high optical transmittance (59%–81%), superior electrochemical impedance (5.4–18.4 $\Omega \cdot cm^2$), and excellent sheet resistance (5.6–14.1 $\Omega \cdot sq^{-1}$) (Figure 8c) [114]. The hybrid structures retained the superior mechanical properties of flexible metal grids other than brittle ITO, with no changes in sheet resistance even after 5000 bending cycles. Simple lithography and wet etching were applied. By controlling the parameters of ITO/gold grid hybrid structure, high optical transmittance, excellent electrochemical performance and mechanical flexibility were obtained. The flexible and transparent ITO/metal grid microelectrodes and interconnects can promote the new experimental designs combining electrophysiology and optophysiology, and serve as the next generation multifunctional optoelectronic neural interfaces.

Another carbon-based material for interconnects is the carbon fiber (CF). Maria et al. introduced a microfabrication technique for patterning flexible, cloth-like, polymer-derived CF mats embedded in polyimide (PI) by selective reactive ion etching (Figure 8d) [115]. This scalable, monolithic manufacturing method eliminated any joints or metal interconnects and created ECoG electrode arrays based on a single CF mat. The resolution of the CF structure was as low as 12.5 μm in-plane and height of about 3 μm. A combination of

photolithography, stripping, and etching were used to embed the carbon fiber mat and form a pattern. These super-flexible neural interfaces show mechanical and electrochemical stability and magnetic resonance compatibility in vitro, as well as excellent recording performance in vivo. In this work, the patterning processing for carbon fibers provides as a valuable alternative method for other carbon-based flexible devices.

Electrodes bearing large stretching meet the problem of easy delamination of electodes from the substrate due to the mechanical mismatch. Qi et al. prepared polypyrrole (PPy) electrode materials modified by nanowires through a simple electro-polymerization process (Figure 8e) [116]. An effective way to acquire stretchable electrode is to induce wavy structure on electrode surface by pre-stretching strategy. A transition layer was constructed at the electrode-substrate interface to enhance the adhesion between electrode array and substrate. By utilizing the PPy as the conductive electrode, stretchable polymeric MEAs were fabricated with both high stretchability (≈100%) and good electrode–substrate adhesive strength (1.9 MPa). Furthermore, low Young′s modulus (450 kPa), excellent cycling stability (10,000 cycles), and high conductivity of the MEAs were also achieved for ECoG signal acquiring.

With the development of 3D printing, the fabrication of thin-film electrodes with various structures has been greatly simplified. Hyunwoo et al. introduced a novel 3D printable conducting polymer ink based on poly(3,4-ethylenedioxythiophene):polystyrene sulfonate (PEDOT:PSS) for 3D printing of conducting polymers, and even a soft neural probe (Figure 8f) [77]. Conductive polymer ink was prepared from PEDOT:PSS solution, dried at 60 °C for 24 h after printing followed by annealing at 130 °C for many times. The Young's modulus of 3D printable conductive polymer ink reached about 1.5 GPa in dry state and reduced by three orders of magnitude in hydrogel state, effectively improving the mechanical matching degree between devices and brain tissue.

Silver nanowires have excellent electrical conductivity and mechanical properties, which are generally used to make conductive structures of thin-film neural electrodes in recent years. Silver nanowires also provide good transparency. Teppei et al. reported the material strategy underlying an optogenetic neural interface comprising stretchable and transparent conductive tracks and capable of demonstrating high biocompatibility after long-term (5 months) implantation. Ag/Au core-shell nanowires contribute toward improving track performance in terms of stretchability (<60% strain), transparency (<83%) and electrical resistance (15 $\Omega \cdot sq^{-1}$) (Figure 8g) [117]. Stretchable transparent silver nanowires/gold nanowires are encapsulated in transparent polymer and connected to hydrogel-coated microelectrodes through silver pads. Transparent traces have 3 times higher stretchability and 20 times higher electrical durability compared to pristine silver nanowires. The high transparence and noble metal behavior will help reduce the light-induced artifacts for optogenetic analyses. Ag/Au core-shell nanowires show lower cytotoxicity and inflammatory reactions than traditional metal interconnects, which are expected to become a substitute for traditional metals.

Good tensile properties can help conductive materials better adapt to the overall deformation of the electrode and the brain. Wen et al. proposed a multifunctional, flexible, and stretchable neural probe for chemical sensing and chemical delivery using gallium (Ga) in the probe construction (Figure 8h) [81]. The multifunctional and ultra-large adjustable stiffness probe was a compact multi-layer independent structure, which integrated platinum electrodes, microfluidic channels, and electrical interconnections. The stiffness of this probe could be adjusted by five orders of magnitude before and after brain insertion, without external shuttle vector during implantation. Liquid gallium was injected into interconnection and hardened channels, and frozen to solid state to maintain shape and strength. Once implanted in the body, the probe became ultrasoft in a few minutes. Using miniaturized design and soft base material, the flexible and stretchable probe had less tissue damage induced by brain movement in all directions.

4. Conclusions and Recommendations

Recent advances and substantial achievements on implantable thin film devices as BCI can address the issues of mechanical interfacial mismatch owing to material properties and delicate structures, and reduce the damage to the brain tissue for chronic implantation.

In this brief review, different types of flexible thin film electrodes were introduced according to their structure layouts and fabrication processes. They will improve functional characteristics of neural electrodes with brain-compatible mechanical properties, low invasiveness, light transmission, high resolution, biodegradation, and so forth. Four typical structure layouts were proposed to fit either the cortical surface or the deep brain, including the plane, mesh, probe, and microwire. The fabrication processes were then discussed according to the high resolution, special substrates, and interconnect materials. Advanced processing methods, such as electron beam lithography, 3D printing, and hot drawing, were compared with traditional lithography. The processing technologies of special substrates and unconventional conductive materials were also discussed, given the compatibility to MEMS fabrication. Biodegradable materials have good biocompatibility and minimal tissue damage, which will gradually dissolve in vivo after a few days to a month without the need of secondary operation. Conductive materials, such as liquid metal, PEDOT:PSS, and gold/silver nanowires, were also used as an alternative to common metal films.

Although flexible thin film electrodes such as BCI have made significant advances recently, there remains challenges to improve the compliance, prolong the service life, reduce the electrode size, and increase the density. The potential difficulties mainly focus on the following three aspects: (1) New insulating and conductive materials with unique properties or functions are usually incompatible with the existing processing technologies; (2) The brain injury caused by implantable devices is inevitable, especially for the insertion case; (3) Compared with the massive neurons in the whole brain, the number of electrode sites is too small, and they can only focus on a limited local area with little information.

The future development of flexible thin film devices as implantable BCI should concentrate on the above-mentioned issues, and address them by the continuous improvement of structural optimization and fabrication compatibility based on the advanced materials. In order to reduce the mechanical trauma caused by the insertion and brain micromotion, we should explore neural probes with adjustable strength and flexibility, further miniaturize the electrode size and improve the mechanical matching between the implanted device and the brain tissue. With suitable materials, the chemical stability can be further improved to promote the biocompatibility of electrode-tissue interface, enhance the quality of recording signals, and inhibit tissue damage during neural stimulation, so as to realize stable chronic implantation with superior performance. In the future, flexible thin film brain-computer interfaces will be more diversified as a fundamental tool to interact with brain information. We envision that the implantable thin film devices will continue to be crucial for neural engineering and neuroscience. Meanwhile, breakthrough innovations are needed to address key technical challenges.

Author Contributions: Writing-Original Draft Preparation, Y.Z. and B.J.; Writing-Review & Editing, Y.Z., B.J., S.H., H.F., and H.C.; Visualization & Supervision, M.W., K.Z. and X.Y.; Project Administration, B.J. and X.Y.; Funding Acquisition, B.J. and M.W.; All authors contribute to organize papers and write the manuscript. All authors have read and agreed to the published version of the manuscript.

Funding: This research was funded by China Postdoctoral Science Foundation (2020TQ0246), the Fundamental Research Funds for the Central Universities (31020200QD013) and the Fundamental Research Funds for the Provincial Universities of Zhejiang (GK199900X001).

Institutional Review Board Statement: Not applicable.

Informed Consent Statement: Not applicable.

Acknowledgments: The authors thank to partial financial support from the project funded by China Postdoctoral Science Foundation (2020TQ0246), the Fundamental Research Funds for the Central

Universities (31020200QD013) and the Fundamental Research Funds for the Provincial Universities of Zhejiang (GK199900X001).

Conflicts of Interest: The authors declare no conflict of interest.

References

1. Birbaumer, N. Breaking the silence: Brain–computer interfaces (BCI) for communication and motor control. *Psychophysiology* **2006**, *43*, 517–532. [CrossRef]
2. Perlmutter, J.S.; Mink, J.W. Deep brain stimulation. *Annu. Rev. Neurosci.* **2006**, *29*, 229–257. [CrossRef]
3. Fetz, E. Restoring motor function with bidirectional neural interfaces. *Prog. Brain Res.* **2015**, *218*, 241–252.
4. Maharbiz, M.M.; Muller, R.; Alon, E.; Rabaey, J.M.; Carmena, J.M. Reliable next-generation cortical interfaces for chronic brain–machine interfaces and neuroscience. *Proc. IEEE* **2016**, *105*, 73–82. [CrossRef]
5. Benabid, A.L.; Costecalde, T.; Eliseyev, A.; Charvet, G.; Verney, A.; Karakas, S.; Foerster, M.; Lambert, A.; Morinière, B.; Abroug, N.; et al. An exoskeleton controlled by an epidural wireless brain–machine interface in a tetraplegic patient: A proof-of-concept demonstration. *Lancet Neurol.* **2019**, *18*, 1112–1122. [CrossRef]
6. Ganzer, P.D.; Colachis, S.C.; Schwemmer, M.A.; Friedenberg, D.A.; Dunlap, C.F.; Swiftney, C.E.; Jacobowitz, A.F.; Weber, D.J.; Bockbrader, M.A.; Sharma, G. Restoring the sense of touch using a sensorimotor demultiplexing neural interface. *Cell* **2020**, *181*, 763–773. [CrossRef] [PubMed]
7. Engel, A.K.; Moll, C.K.E.; Fried, I.; Ojemann, G.A. Invasive recordings from the human brain: Clinical insights and beyond. *Nat. Rev. Neurosci.* **2005**, *6*, 35–47. [CrossRef] [PubMed]
8. Dimitriadis, G.; Fransen AM, M.; Maris, E. Sensory and cognitive neurophysiology in rats, Part 1: Controlled tactile stimulation and micro-ECoG recordings in freely moving animals. *J. Neurosci. Methods* **2014**, *232*, 63–73. [CrossRef] [PubMed]
9. Yang, T.; Hakimian, S.; Schwartz, T.H. Intraoperative Electro CorticoGraphy (ECog): Indications, techniques, and utility in epilepsy surgery. *Epileptic Disord* **2014**, *16*, 271–279.
10. Ji, B.; Ge, C.; Guo, Z.; Wang, L.; Wang, M.; Xie, Z.; Xu, Y.; Li, H.; Yang, B.; Wang, X.; et al. Flexible and stretchable opto-electric neural interface for low-noise electrocorticogram recordings and neuromodulation in vivo. *Biosens. Bioelectron.* **2020**, *153*, 112009. [CrossRef]
11. Li, X.; Song, Y.; Xiao, G.; Xie, J.; Dai, Y.; Xing, Y.; He, E.; Wang, Y.; Xu, S.; Zhang, L.; et al. Flexible electrocorticography electrode array for epileptiform electrical activity recording under glutamate and GABA modulation on the primary somatosensory cortex of rats. *Micromachines* **2020**, *11*, 732. [CrossRef] [PubMed]
12. Wu, F.; Stark, E.; Ku, P.-C.; Wise, K.D.; Buzsáki, G.; Yoon, E. Monolithically integrated μLEDs on silicon neural probes for high-resolution optogenetic studies in behaving animals. *Neuron* **2015**, *88*, 1136–1148. [CrossRef]
13. Jun, J.J.; Steinmetz, N.A.; Siegle, J.H.; Denman, D.J.; Bauza, M.; Barbarits, B.; Lee, A.K.; Anastassiou, C.A.; Andrei, A.; Aydın, Ç.; et al. Fully integrated silicon probes for high-density recording of neural activity. *Nature* **2017**, *551*, 232–236. [CrossRef] [PubMed]
14. Chung, J.E.; Joo, H.R.; Fan, J.L.; Liu, D.F.; Barnett, A.H.; Chen, S.; Geaghan-Breiner, C.; Karlsson, M.P.; Karlsson, M.; Lee, K.Y.; et al. High-density, long-lasting, and multi-region electrophysiological recordings using polymer electrode arrays. *Neuron* **2019**, *101*, 21–31. [CrossRef]
15. Sahasrabuddhe, K.; Khan, A.A.; Singh, A.P.; Stern, T.M.; Ng, Y.; Tadić, A.; Orel, P.; LaReau, C.; Pouzzner, D.; Nishimura, K.; et al. The Argo: A 65,536 channel recording system for high density neural recording in vivo. *bioRxiv* **2020**. [CrossRef]
16. Obaid, A.; Hanna, M.-E.; Wu, Y.-W.; Kollo, M.; Racz, R.; Angle, M.R.; Müller, J.; Brackbill, N.; Wray, W.; Franke, F.; et al. Massively parallel microwire arrays integrated with CMOS chips for neural recording. *Sci. Adv.* **2020**, *6*, eaay2789. [CrossRef]
17. Canales, A.; Jia, X.; Froriep, U.P.; Koppes, R.A.; Tringides, C.M.; Selvidge, J.; Lu, C.; Hou, C.; Wei, L.; Fink, Y.; et al. Multifunctional fibers for simultaneous optical, electrical and chemical interrogation of neural circuits in vivo. *Nat. Biotechnol.* **2015**, *33*, 277–284. [CrossRef] [PubMed]
18. Kim, T.-I.; McCall, J.G.; Jung, Y.H.; Huang, X.; Siuda, E.R.; Li, Y.; Song, J.; Song, Y.M.; Pao, H.A.; Kim, R.-H.; et al. Injectable, cellular-scale optoelectronics with applications for wireless optogenetics. *Science* **2013**, *340*, 211–216. [CrossRef]
19. Zhang, J.; Laiwalla, F.; Kim, J.A.; Urabe, H.; Wagenen, R.V.; Song, Y.K.; Connors, B.W.; Feng, Z.; Deisseroth, K.; Nurmikko, A.V. Integrated device for optical stimulation and spatiotemporal electrical recording of neural activity in light-sensitized brain tissue. *J. Neural Eng.* **2009**, *6*, 055007. [CrossRef] [PubMed]
20. Kim, D.; Yokota, T.; Suzuki, T.; Lee, S.; Someya, T. Ultraflexible organic light-emitting diodes for optogenetic nerve stimulation. *Proc. Natl. Acad. Sci. USA* **2020**, *117*, 21138–21146. [CrossRef] [PubMed]
21. Johnson, L.A.; Wander, J.D.; Sarma, D.; Lee, S.; Someya, T. Direct electrical stimulation of the somatosensory cortex in humans using electrocorticography electrodes: A qualitative and quantitative report. *J. Neural Eng.* **2013**, *10*, 036021. [CrossRef] [PubMed]
22. Hughes, C.L.; Flesher, S.N.; Weiss, J.M.; Downey, J.E.; Collinger, J.L.; Gaunt, R.A. Neural stimulation and recording performance in human somatosensory cortex over 1500 days. *medRxiv* **2020**. [CrossRef]
23. Parastarfeizabadi, M.; Kouzani, A.Z. Advances in closed-loop deep brain stimulation devices. *J. Neuroeng. Rehabil.* **2017**, *14*, 79. [CrossRef]
24. Bonmassar, G.; Lee, S.W.; Freeman, D.K.; Polasek, M.; Gale, J.T. Microscopic magnetic stimulation of neural tissue. *Nat. Commun.* **2012**, *3*, 1–10. [CrossRef]

25. Lee, S.W.; Fallegger, F.; Casse, B.D.F.; Fried, S.I. Implantable microcoils for intracortical magnetic stimulation. *Sci. Adv.* **2016**, *2*, e1600889. [CrossRef] [PubMed]
26. Lee, H.E.; Park, J.H.; Jang, D.; Shin, J.H.; Hwang, G.T. Optogenetic brain neuromodulation by stray magnetic field via flash-enhanced magneto-mechano-triboelectric nanogenerator. *Nano Energy* **2020**, *75*, 104951. [CrossRef]
27. Lee, H.J.; Son, Y.; Kim, J.; Lee, C.J.; Yoon, E.S.; Cho, I.J. A multichannel neural probe with embedded microfluidic channels for simultaneous in vivo neural recording and drug delivery. *Lab Chip* **2015**, *15*, 1590–1597. [CrossRef] [PubMed]
28. Jeong, J.W.; McCall, J.G.; Shin, G.; Zhang, Y.; Al-Hasani, R.; Kim, M.; Li, S.; Sim, J.Y.; Jang, K.; Shi, Y.; et al. Wireless optofluidic systems for programmable in vivo pharmacology and optogenetics. *Cell* **2015**, *162*, 662–674. [CrossRef]
29. Dagdeviren, C.; Ramadi, K.B.; Joe, P.; Spencer, K.; Schwerdt, H.N.; Shimazu, H.; Delcasso, S.; Amemori, K.; Nunez-Lopez, C.; Graybiel, A.M.; et al. Miniaturized neural system for chronic, local intracerebral drug delivery. *Sci. Transl. Med.* **2018**, *10*, 425. [CrossRef]
30. Bruno, G.; Colistra, N.; Melle, G.; Cerea, A.; Dipalo, M. Microfluidic multielectrode arrays for spatially localized drug delivery and electrical recordings of primary neuronal cultures. *Front. Bioeng. Biotechnol.* **2020**, *8*, 626. [CrossRef]
31. Cotler, M.J.; Rousseau, E.B.; Ramadi, K.B.; Fang, J.; Graybiel, A.M.; Langer, R.; Cima, M.J. Steerable microinvasive probes for localized drug delivery to deep tissue. *Small* **2019**, *15*, 1901459. [CrossRef]
32. Maynard, E.M.; Nordhausen, C.T.; Normann, R.A. The Utah intracortical electrode array: A recording structure for potential brain-computer interfaces. *Electroencephalogr. Clin. Neurophysiol.* **1997**, *102*, 228–239. [CrossRef]
33. Rousche, P.J.; Normann, R.A. Chronic recording capability of the Utah intracortical electrode array in cat sensory cortex. *J. Neurosci. Methods* **1998**, *82*, 1–15. [CrossRef]
34. Normann, R.A.; Fernandez, E. Clinical applications of penetrating neural interfaces and Utah electrode array technologies. *J. Neural Eng.* **2016**, *13*, 061003. [CrossRef] [PubMed]
35. Kipke, D.R.; Vetter, R.J.; Williams, J.C.; Hetke, J.F. Silicon-substrate intracortical microelectrode arrays for long-term recording of neuronal spike activity in cerebral cortex. *IEEE Trans. Neural Syst. Rehabil. Eng.* **2003**, *11*, 151–155. [CrossRef] [PubMed]
36. Vetter, R.J.; Williams, J.C.; Hetke, J.F.; Nunamaker, E.A.; Kipke, D.R. Chronic neural recording using silicon-substrate microelectrode arrays implanted in cerebral cortex. *IEEE Trans. Biomed. Eng.* **2004**, *51*, 896–904. [CrossRef]
37. Ruther, P.; Herwik, S.; Kisban, S.; Seidl, K.; Paul, O. Recent progress in neural probes using silicon MEMS technology. *IEEE Trans. Electr. Electron. Eng.* **2010**, *5*, 505–515. [CrossRef]
38. Wang, M.H.; Gu, X.W.; Ji, B.W.; Wang, L.C.; Guo, Z.J.; Yang, B.; Wang, X.L.; Li, C.Y.; Liu, J.Q. Three-dimensional drivable optrode array for high-resolution neural stimulations and recordings in multiple brain regions. *Biosens. Bioelectron.* **2019**, *131*, 9–16. [CrossRef]
39. Hubel, D.H. Tungsten microelectrode for recording from single units. *Science* **1957**, *125*, 549–550. [CrossRef] [PubMed]
40. Tseng, W.T.; Yen, C.T.; Tsai, M.L. A bundled microwire array for long-term chronic single-unit recording in deep brain regions of behaving rats. *J. Neurosci. Methods* **2011**, *201*, 368–376. [CrossRef]
41. Zhao, S.; Liu, X.; Xu, Z.; Ren, H.; Deng, B.; Tang, M.; Lu, L.; Fu, X.; Peng, H.; Liu, Z. Graphene encapsulated copper microwires as highly MRI compatible neural electrodes. *Nano Lett.* **2016**, *16*, 7731–7738. [CrossRef]
42. Elkin Benjamin, S.; Azeloglu, E.U.; Costa, K.D.; Morrison, B. Mechanical heterogeneity of the rat hippocampus measured by atomic force microscope indentation. *J. Neurotrauma* **2007**, *24*, 812–822. [CrossRef]
43. Budday, S.; Nay, R.; De Rooij, R.; Steinmann, P.; Wyrobek, T.; Ovaert, T.C.; Kuhl, E. Mechanical properties of gray and white matter brain tissue by indentation. *J. Mech. Behav. Biomed. Mater.* **2015**, *46*, 318–330. [CrossRef]
44. Biran, R.; Martin, D.C.; Tresco, P.A. Neuronal cell loss accompanies the brain tissue response to chronically implanted silicon microelectrode arrays. *Exp. Neurol.* **2005**, *195*, 115–126. [CrossRef] [PubMed]
45. Lee, H.; Bellamkonda, R.V.; Sun, W.; Levenston, M.E. Biomechanical analysis of silicon microelectrode-induced strain in the brain. *J. Neural Eng.* **2005**, *2*, 81–89. [CrossRef] [PubMed]
46. Polikov, V.S.; Tresco, P.A.; Reichert, W.M. Response of brain tissue to chronically implanted neural electrodes. *J. Neurosci. Methods* **2005**, *148*, 1–18. [CrossRef] [PubMed]
47. Köhler, P.; Wolff, A.; Ejserholm, F.; Wallman, L.; Schouenborg, J.; Linsmeier, C.E. Influence of probe flexibility and gelatin embedding on neuronal density and glial responses to brain implants. *PLoS ONE* **2015**, *10*, e0119340. [CrossRef]
48. Williams, J.C.; Hippensteel, J.A.; Dilgen, J. Complex impedance spectroscopy for monitoring tissue responses to inserted neural implants. *J. Neural Eng.* **2007**, *4*, 410. [CrossRef] [PubMed]
49. Musk, E. Neuralink an integrated brain-machine interface platform with thousands of channels. *J. Med. Internet Res.* **2019**, *21*, e16194. [CrossRef] [PubMed]
50. Du, Z.J.; Kolarcik, C.L.; Kozai, T.D.; Luebben, S.D.; Sapp, S.A.; Zheng, X.S.; Nabity, J.A.; Cui, X.T. Ultrasoft microwire neural electrodes improve chronic tissue integration. *Acta Biomater.* **2017**, *53*, 46–58. [CrossRef]
51. Luan, L.; Wei, X.; Zhao, Z.; Siegel, J.J.; Potnis, O.; Tuppen, C.A.; Lin, S.; Kazmi, S.; Fowler, R.A.; Holloway, S.; et al. Ultraflexible nanoelectronic probes form reliable, glial scar–free neural integration. *Sci. Adv.* **2017**, *3*, e1601966. [CrossRef]
52. Vomero, M.; Cruz, M.F.P.; Zucchini, E.; Ciarpella, F.; Delfino, E.; Carli, S.; Boehler, C.; Asplund, M.; Ricci, D.; Fadiga, L.; et al. Conformable polyimide-based μECoGs: Bringing the electrodes closer to the signal source. *Biomaterials* **2020**, *255*, 120178. [CrossRef] [PubMed]

53. Wang, X.; Hirschberg, A.W.; Xu, H.; Slingsby-Smith, Z.; LeComte, A.; Scholten, K.; Song, D.; Meng, E. A Parylene neural probe array for multi-region deep brain recordings. *J. Microelectromechanical Syst.* **2020**, *29*, 499–513. [CrossRef]
54. Zatonyi, A.; Madarasz, M.; Szabo, G.; Lrincz, T.; Fekete, Z. Transparent, low-autofluorescence microECoG device for simultaneous Ca^{2+} imaging and cortical electrophysiology in vivo. *J. Neural Eng.* **2020**, *17*, 016062. [CrossRef]
55. Fu, T.M.; Hong, G.; Viveros, R.D.; Zhou, T.; Lieber, C.M. Highly scalable multichannel mesh electronics for stable chronic brain electrophysiology. *Proc. Natl. Acad. Sci. USA* **2017**, *114*, E10046–E10055. [CrossRef] [PubMed]
56. Park, A.H.; Lee, S.H.; Lee, C.; Kim, J.; Lee, H.E.; Paik, S.B.; Lee, J. Optogenetic mapping of functional connectivity in freely moving mice via insertable wrapping electrode array beneath the skull. *ACS Nano* **2016**, *10*, 2791–2802. [CrossRef]
57. Byun, S.H.; Sim, J.Y.; Zhou, Z.; Lee, J.; Jeong, J.W. Mechanically transformative electronics, sensors, and implantable devices. *Sci. Adv.* **2019**, *5*, eaay0418. [CrossRef]
58. Jimbo, Y.; Matsuhisa, N.; Lee, W.; Zalar, P.; Jinno, H.; Yokota, T.; Sekino, M.; Someya, T. Ultraflexible transparent oxide/metal/oxide stack electrode with low sheet resistance for electrophysiological measurements. *ACS Appl. Mater. Interfaces* **2017**, *9*, 34744–34750. [CrossRef]
59. Liu, X.; Lu, Y.; Ege, I.; Shi, Y.; Duygu, K. A compact closed-loop optogenetics system based on artifact-free transparent graphene electrodes. *Front. Neurosci.* **2018**, *12*, 132. [CrossRef]
60. Yamagiwa, S.; Ishida, M.; Kawano, T. Flexible optrode array: Parylene-film waveguide arrays with microelectrodes for optogenetics. In *2015 Transducers-2015 18th International Conference on Solid-State Sensors, 63 Actuators and Microsystems (TRANSDUCERS)*; IEEE: Piscataway, NJ, USA, 2015; pp. 277–280.
61. Reddy, J.W.; Lassiter, M.; Chamanzar, M. Parylene photonics: A flexible, broadband optical waveguide platform with integrated micromirrors for biointerfaces. *Microsystems Nanoeng.* **2020**, *6*, 1–14. [CrossRef]
62. Kwon, K.Y.; Sirowatka, B.; Weber, A.; Li, W. Opto-μECoG array: A hybrid neural interface with transparent μECoG electrode array and integrated LEDs for optogenetics. *IEEE Trans. Biomed. Circuits Syst.* **2013**, *7*, 593–600. [CrossRef]
63. Ji, B.; Guo, Z.; Wang, M.; Yang, B.; Wang, X.; Li, W.; Liu, J. Flexible polyimide-based hybrid opto-electric neural interface with 16 channels of micro-LEDs and electrodes. *Microsyst. Nanoeng.* **2018**, *4*, 1–11. [CrossRef]
64. Guan, S.; Wang, J.; Gu, X.; Zhao, Y.; Hou, R.; Fan, H.; Zou, L.; Gao, L.; Du, M.; Li, C. Elastocapillary self-assembled neurotassels for stable neural activity recordings. *Sci. Adv.* **2019**, *5*, eaav2842. [CrossRef]
65. Zhou, H.L.; Zhang, Y.; Qiu, Y.; Wu, H.P.; Qin, W.Y.; Liao, Y.B.; Yu, Q.; Cheng, H.Y. Stretchable piezoelectric energy harvesters and self-powered sensors for wearable and implantable devices. *Biosens. Bioelectron.* **2020**, *168*, 112569. [CrossRef] [PubMed]
66. Morikawa, Y.; Ayub, S.; Paul, O.; Kawano, T.; Ruther, P. Highly stretchable kirigami structure with integrated LED chips and electrodes for optogenetic experiments on perfused hearts. In *2019 20th International Conference on Solid-State Sensors, Actuators and Microsystems & Eurosensors XXXIII (TRANSDUCERS & EUROSENSORS XXXIII)*; IEEE: Piscataway, NJ, USA, 2019; pp. 2484–2487.
67. Vahidi, N.W.; Rudraraju, S.; Castagnola, E.; Cea, C.; Nimbalkar, S.; Hanna, R.; Arvizu, R.; A Dayeh, S.; Gentner, T.Q.; Kassegne, S. Epi-Intra neural probes with glassy carbon microelectrodes help elucidate neural coding and stimulus encoding in 3D volume of tissue. *J. Neural Eng.* **2020**, *17*, 046005. [CrossRef] [PubMed]
68. Khodagholy, D.; Gelinas, J.N.; Thesen, T.; Doyle, W.K.; Devinsky, O.; Malliaras, G.G.; Buzsáki, G. NeuroGrid: Recording action potentials from the surface of the brain. *Nat. Neurosci.* **2015**, *18*, 310–315. [CrossRef]
69. Viventi, J.; Kim, D.-H.; Vigeland, L.; Frechette, E.S.; Blanco, J.A.; Kim, Y.-S.; Avrin, A.E.; Tiruvadi, V.R.; Hwang, S.-W.; Vanleer, A.C.; et al. Flexible, foldable, actively multiplexed, high-density electrode array for mapping brain activity in vivo. *Nat. Neurosci.* **2011**, *14*, 1599–1605. [CrossRef] [PubMed]
70. Woods, V.; Trumpis, M.; Bent, B.; Palopoli-Trojani, K.; Chiang, C.-H.; Wang, C.; Yu, C.; Insanally, M.N.; Froemke, R.C.; Viventi, J. Long-term recording reliability of liquid crystal polymer μECoG arrays. *J. Neural Eng.* **2018**, *15*, 066024. [CrossRef] [PubMed]
71. Shi, J.; Fang, Y. Flexible and implantable microelectrodes for chronically stable neural interfaces. *Adv. Mater.* **2019**, *31*, e1804895. [CrossRef] [PubMed]
72. Tybrandt, K.; Khodagholy, D.; Dielacher, B.; Stauffer, F.; Renz, A.F.; Buzsáki, G.; Vörös, J. High-density stretchable electrode grids for chronic neural recording. *Adv. Mater.* **2018**, *30*, e1706520. [CrossRef]
73. Liu, J.; Fu, T.M.; Cheng, Z.; Hong, G.S.; Zhou, T. Syringe-injectable electronics. *Nat. Nanotechnol.* **2015**, *10*, 629–636. [CrossRef]
74. Kim, D.-H.; Viventi, J.; Amsden, J.J.; Xiao, J.; Vigeland, L.; Kim, Y.-S.; Blanco, J.A.; Panilaitis, B.; Frechette, E.S.; Contreras, D.; et al. Dissolvable films of silk fibroin for ultrathin conformal bio-integrated electronics. *Nat. Mater.* **2010**, *9*, 511–517. [CrossRef] [PubMed]
75. Zhao, Z.; Li, X.; He, F.; Wei, X.; Lin, S.; Xie, C. Parallel, minimally-invasive implantation of ultra-flexible neural electrode arrays. *J. Neural Eng.* **2019**, *16*, 035001. [CrossRef]
76. Wang, K.; Frewin, C.L.; Esrafilzadeh, D.; Yu, C.; Wang, C.; Pancrazio, J.J.; Romero-Ortega, M.; Jalili, R.; Wallace, G. High-performance graphene-fiber-based neural recording microelectrodes. *Adv. Mater.* **2019**, *31*, 1805867. [CrossRef] [PubMed]
77. Yuk, H.; Lu, B.; Lin, S.; Qu, K.; Xu, J.; Luo, J.; Zhao, X. 3D printing of conducting polymers. *Nat. Commun.* **2020**, *11*, 1–8. [CrossRef]
78. Yang, J.; Du, M.; Wang, L.; Li, S.; Wang, G.; Yang, X.; Zhang, L.; Fang, Y.; Zheng, W.; Yang, G.; et al. Bacterial cellulose as a supersoft neural interfacing substrate. *ACS Appl. Mater. Interfaces* **2018**, *10*, 33049–33059. [CrossRef] [PubMed]
79. Yu, K.J.; Kuzum, D.; Hwang, S.W.; Kim, B.H.; Juul, H.; Kim, N.H.; Won, S.M.; Chiang, K.; Trumpis, M.; Richardson, A.G. Bioresorbable silicon electronics for transient spatiotemporal mapping of electrical activity from the cerebral cortex. *Nat. Mater.* **2016**, *15*, 782–791. [CrossRef] [PubMed]

80. Park, D.-W.; Schendel, A.A.; Mikael, S.; Brodnick, S.K.; Richner, T.J.; Ness, J.P.; Hayat, M.R.; Atry, F.; Frye, S.T.; Pashaie, R.; et al. Graphene-based carbon-layered electrode array technology for neural imaging and optogenetic applications. *Nat. Commun.* **2014**, *5*, 5258. [CrossRef]
81. Ximiao, W.; Wang, B.; Huang, S.; Liu, T.L.; Lee, M.S.; Chung, P.S.; Chow, Y.T.; Huang, I.W.; Monbouquette, H.G.; Maidment, N.T.; et al. Flexible, multifunctional neural probe with liquid metal enabled, ultra-large tunable stiffness for deep-brain chemical sensing and agent delivery. *Biosens. Bioelectron.* **2019**, *131*, 37–45.
82. Seo, K.J.; Artoni, P.; Qiang, Y.; Han, X.; Shi, Z.; Yao, W.H.; Fagiolini, M.; Fang, H. Transparent, flexible, penetrating microelectrode arrays with capabilities of single-unit electrophysiology. *Adv. Biosyst.* **2019**, *3*, 1800276. [CrossRef]
83. Ferro, M.; Proctor, C.M.; Gonzalez, A.; Zhao, E.; Melosh, N.A. NeuroRoots, a bio-inspired, seamless brain machine interface device for long-term recording. *BioRxiv* **2018**. [CrossRef]
84. Ganji, M.; Kaestner, E.; Hermiz, J.; Rogers, N.; Tanaka, A.; Cleary, D.; Lee, S.H.; Snider, J.; Halgren, M.; Cosgrove, G.R.; et al. Development and translation of PEDOT:PSS microelectrodes for intraoperative monitoring. *Adv. Funct. Mater.* **2018**, *28*. [CrossRef]
85. Seo, J.; Kim, K.; Kim, M.K.; Jeong, S.; Kim, H.; Ghim, J.; Lee, J.H.; Choi, N.; Lee, J.; Lee, H.J. Artifact-free 2D mapping of neural activity in vivo through transparent gold nanonetwork array. *Adv. Funct. Mater.* **2020**, *30*, 2000896. [CrossRef]
86. Renz, A.F.; Lee, J.; Tybrandt, K.; Brzezinski, M.; Lorenzo, D.A.; Cheraka, M.C.; Lee, J.; Helmchen, F.; Vörös, J.; Lewis, C.M. Opto-E-Dura: A soft, stretchable ECoG array for multimodal, multiscale neuroscience. *Adv. Heal. Mater.* **2020**, *9*, 2000814. [CrossRef] [PubMed]
87. Ji, B.; Xie, Z.; Hong, W.; Jiang, C.; Guo, Z.; Wang, L.; Wang, X.; Yang, B.; Liu, J. Stretchable parylene-C electrodes enabled by serpentine structures on arbitrary elastomers by silicone rubber adhesive. *J. Materiomics* **2020**, *6*, 330–338. [CrossRef]
88. Chiang, C.-H.; Sang, M.W.; Orsborn, A.L.; Yu, K.J.; Trumpis, M.; Bent, B.; Wang, C.; Xue, Y.; Min, S.; Woods, V. Development of a neural interface for high-definition, long-term recording in rodents and nonhuman primates. *Sci. Transl. Med.* **2020**, *12*, eaay4682. [CrossRef] [PubMed]
89. Insanally, M.; Trumpis, M.; Wang, C.; Chiang, C.H.; Woods, V.; Palopoli-Trojani, K.; Bossi, S.; Froemke, R.; Viventi, J. A low-cost, multiplexed μECoG system for high-density recordings in freely moving rodents. *J. Neural Eng.* **2016**, *13*, 026030. [CrossRef]
90. Shi, Z.; Zheng, F.M.; Zhou, Z.T.; Li, M.; Fan, Z.; Ye, H.P.; Zhang, S.; Xiao, T.; Chen, L.; Tao, T.H.; et al. Silk-enabled conformal multifunctional bioelectronics for investigation of spatiotemporal epileptiform activities and multimodal neural encoding/decoding. *Adv. Sci.* **2019**, *6*, 1801617. [CrossRef] [PubMed]
91. Masvidal-Codina, E.; Illa, X.; Dasilva, M.; Calia, A.B.; Dragojević, T.; Vidal-Rosas, E.E.; Prats-Alfonso, E.; Martínez-Aguilar, J.; Cruz, J.M.D.; Garcia-Cortadella, R.; et al. High-resolution mapping of infraslow cortical brain activity enabled by graphene microtransistors. *Nat. Mater.* **2019**, *18*, 280–288. [CrossRef]
92. Garcia-Cortadella, R.; Schäfer, N.; Cisneros-Fernandez, J.; Ré, L.; Illa, X.; Schwesig, G.; Moya, A.; Santiago, S.; Guirado, G.; Villa, R.; et al. Switchless multiplexing of graphene active sensor arrays for brain mapping. *Nano Lett.* **2020**, *20*, 3528–3537. [CrossRef]
93. Fukushima, M.; Saunders, R.C.; Mullarkey, M.; Doyle, A.M.; Mishkin, M.; Fujii, N. An electrocorticographic electrode array for simultaneous recording from medial, lateral, and intrasulcal surface of the cortex in macaque monkeys. *J. Neurosci. Methods* **2014**, *233*, 155–165. [CrossRef] [PubMed]
94. Kaiju, T.; Keiichi, D.; Masashi, Y.; Kei, W.; Masato, I.; Hiroshi, A.; Kazutaka, T.; Fumiaki, Y.; Masayuki, H.; Takafumi, S. High spatiotemporal resolution ECoG recording of somatosensory evoked potentials with flexible micro-electrode arrays. *Front. Neural Circuits* **2017**, *11*, 20. [CrossRef] [PubMed]
95. Morikawa, Y.; Yamagiwa, S.; Sawahata, H.; Numano, R.; Koida, K.; Ishida, M.; Kawano, T. Ultrastretchable kirigami bioprobes. *Adv. Healthc. Mater.* **2017**, *7*, 1701100. [CrossRef] [PubMed]
96. Xie, C.; Jia, L.; Fu, T.M.; Dai, X.; Wei, Z.; Lieber, C.M. Three-dimensional macroporous nanoelectronic networks as minimally invasive brain probes. *Nat. Mater.* **2015**, *14*, 1286–1292. [CrossRef]
97. Zhang, S.; Wang, C.; Gao, H.; Yu, C.; Song, J. A Removable insertion shuttle for ultraflexible neural probe implantation with stable chronic brain electrophysiological recording. *Adv. Mater. Interfaces* **2020**, *7*, 1901775. [CrossRef]
98. Guo, Z.; Ji, B.; Wang, L.; Yang, B.; Liu, J. A flexible and stretchable kirigami-inspired implantable neural probe with floating microsites for electrophysiology recordings. In *2020 IEEE 33rd International Conference on Micro Electro Mechanical Systems (MEMS)*; IEEE: Piscataway, NJ, USA, 2020; pp. 350–353.
99. Lu, L.; Fu, X.; Liew, Y.; Zhang, Y.; Zhao, S.; Xu, Z.; Zhao, J.; Li, D.; Li, Q.; Stanley, G.B.; et al. Soft and MRI compatible neural electrodes from carbon nanotube fibers. *Nano Lett.* **2019**, *19*, 1577–1586. [CrossRef]
100. Du, M.; Huang, L.; Zheng, J.; Xi, Y.; Dai, Y.; Zhang, W.D.; Yan, W.; Tao, G.M.; Qiu, J.R.; So, K.F.; et al. Flexible fiber probe for efficient neural stimulation and detection. *Adv. Sci.* **2020**, *7*, 2001410. [CrossRef]
101. Wang, L.L.; Xie, Z.X.; Zhong, C.; Tang, Y.Q.; Ye, F.M.; Wang, L.P.; Lu, Y. Self-spreadable Octopus-like Electrode Arrays for Long-term Neural Recordings. *Acta Phys. Chim. Sin.* **2019**. [CrossRef]
102. Scholten, K.; Meng, E. Electron-beam lithography for polymer bioMEMS with submicron features. *Microsyst. Nanoeng.* **2016**, *2*, 16053. [CrossRef] [PubMed]
103. Shim, S.; Park, H.Y.; Choi, G.J.; Shin, H.C.; Kim, S.J. A simply fabricated neural probe by laser machining of a thermally laminated gold thin film on transparent cyclic olefin polymer. *ACS Omega* **2019**, *4*, 2590–2595. [CrossRef]

104. Guo, Y.; Fang, Z.; Du, M.; Yang, L.; Shao, L.; Zhang, X.; Li, L.; Shi, J.; Tao, J.; Wang, J. Flexible and biocompatible nanopaper-based electrode arrays for neural activity recording. *Nano Res.* **2018**, *11*, 5604–5614. [CrossRef]
105. Kedi, X.; Li, S.J.; Dong, S.R.; Zhang, S.M.; Pan, G.; Wang, G.M.; Shi, L.; Guo, W.; Yu, C.N.; Luo, J.K. Bioresorbable electrode array for electrophysiological and pressure signal recording in the brain. *Adv. Healthc. Mater.* **2019**, *8*, 1801649.
106. Chen, C.; Xue, M.M.; Wen, Y.G.; Yao, G.; Cui, Y.; Liao, F.Y.; Yan, Z.C.; Huang, L.; Khan, S.A.; Gao, M.; et al. A ferroelectric ceramic/polymer composite-based capacitive electrode array for in vivo recordings. *Adv. Healthc. Mater.* **2017**, *6*, 1700305. [CrossRef]
107. Ware, T.; Simon, D.; Liu, C.; Musa, T.; Vasudevan, S.; Sloan, A.; Keefer, E.W.; Rennaker, R.L.; Voit, W. Thiol-ene/acrylate substrates for softening intracortical electrodes. *J. Biomed. Mater. Res. Part B Appl. Biomater.* **2014**, *102*, 1–11. [CrossRef]
108. Oribe, S.; Yoshida, S.; Kusama, S.; Osawa, S.I.; Nishizawa, M. Hydrogel-based organic subdural electrode with high conformability to brain surface. *Sci. Rep.* **2019**, *9*, 1–10. [CrossRef] [PubMed]
109. Rihani, R.; Stiller, A.M.; Usoro, J.O.; Lawson, J.; Pancrazio, J.J. Deployable, liquid crystal elastomer-based intracortical probes. *Acta Biomater.* **2020**, *111*, 54–64. [CrossRef]
110. Ware, T.; Simon, D.; Hearon, K.; Liu, C.; Shah, S.; Reeder, J.; Khodaparast, N.; Kilgrad, M.P.; Maitland, D.J.; Rennaker, R.L., II; et al. Three-dimensional flexible electronics enabled by shape memory polymer substrates for responsive neural interfaces. *Macromol. Mater. Eng.* **2012**, *297*, 1193–1202. [CrossRef] [PubMed]
111. Shoffstall, A.J.; Ecker, M.; Danda, V.; Joshi-Imre, A.; Stiller, A.; Yu, M.; Paiz, J.E.; Mancuso, E.; Bedell, H.W.; Voit, W.E.; et al. Characterization of the neuroinflammatory response to thiol-ene shape memory polymer coated intracortical microelectrodes. *Micromachines* **2018**, *9*, 486. [CrossRef]
112. Wang, J.; Zhao, Q.; Wang, Y.; Zeng, Q.; Du, X. Self-unfolding flexible microelectrode arrays based on shape memory polymers. *Adv. Mater. Technol.* **2019**, *4*, 1900566. [CrossRef]
113. Zhang, J.; Liu, X.J.; Xu, W.J.; Luo, W.H.; Li, M. Stretchable transparent electrode arrays for simultaneous electrical and optical interrogation of neural circuits in vivo. *Nano Lett.* **2018**, *18*, 2903–2911. [CrossRef]
114. Chen, Z.; Yin, R.T.; Obaid, S.N.; Tian, J.; Lu, L. Flexible and transparent metal oxide/metal grid hybrid interfaces for electrophysiology and optogenetics. *Adv. Mater. Technol.* **2020**, *5*, 2000322. [CrossRef]
115. Vomero, M.; Gueli, C.; Zucchini, E.; Fadiga, L.; Stieglitz, T. Flexible bioelectronic devices based on micropatterned monolithic carbon fiber materials. *Adv. Mater. Technol.* **2019**, *5*, 1900713. [CrossRef]
116. Qi, D.; Liu, Z.; Liu, Y.; Jiang, Y.; Leow, W.R.; Pal, M.; Pan, S.; Yang, H.; Wang, Y.; Zhang, X. Highly stretchable, compliant, polymeric microelectrode arrays for in vivo electrophysiological interfacing. *Adv. Mater.* **2017**, *29*, 1702800. [CrossRef]
117. Araki, T.; Yoshida, F.; Uemura, T.; Noda, Y.; Sekitani, T. Long-term implantable, flexible, and transparent neural interface based on Ag/Au core–shell nanowires. *Adv. Healthc. Mater.* **2019**, *8*, e1900130. [CrossRef] [PubMed]